OPTIMIZING RESPONSE STRATEGIES TO THE COVID-19 PANDEMIC IN NOVA SCOTIA

by

Melissa Kate Gillis

Submitted in partial fulfillment of the
requirements for the degree of Master of Applied Science

at

Dalhousie University
Halifax, Nova Scotia
August 2021

Dalhousie University is located in Mi'kma'ki, the
ancestral and unceded territory of the Mi'kmaq.
We are all Treaty people.

Table of Contents

List of Tables

List of Figures

Abstract

Epidemics require dynamic response strategies that encompass a multitude of policy alternatives to effectively balance health, economic, and societal considerations. Due to the complexity and wide array of policy alternatives, decision makers require tools to determine effective strategies and assess their impact. This thesis proposes a simulation-optimization framework to aid policymakers select closure, protection, and travel policies to minimize the total number of infections under a limited budget. The proposed framework combines a modified, age-stratified susceptible-exposed-infected-recovered (SEIR) compartmental model to evaluate the health impact of response strategies and two meta-heuristic optimization procedures, namely Genetic Algorithm (GA) and Simulated Annealing (SA), to effectively search for better strategies. Two types of response strategies are considered: time-based and state-based. The former is proactive in nature, prescribing at the outset response policies to be implemented over a set period of time, whereas the latter is a reactive strategy that adjusts the policies based on the number of new infections observed, mimicking the method often used by policymakers. Both frameworks were implemented on a real case study in Nova Scotia to devise optimized response strategies to COVID-19. The two approaches found a clear trade-off between health and economic considerations. The time-based results show regardless of the budget, policy makers should oscillate between policies of varying degrees of strictness. Closure policies seem to be the most sensitive to policy restrictions, followed by travel policies. Results suggest that after a budget threshold is met, practicing social distancing and wearing masks are always recommended. The state-based results set the optimal limits such that restrictions are tightened whenever there are signs of a potential community spread and loosened when the spread is contained. Given the high infectivity of the disease, the lower limits (triggering the shift to less strict policies) are set quite low, ranging between 0 and 20 infections depending on the budget and the existing policies. Both frameworks are generic and can be extended to encompass vaccination policies and to use different epidemiological models or optimization methods. The model was also used to compare potential policy scenarios during the vaccination period, to help determine a suitable timeline for lifting the restrictions while minimizing the public health impact. The test results indicate that masks and social distancing will be required in order to continue to keep the case count and hospitalizations low, even as closure and travel policies are relaxed.

Acknowledgements

Throughout this thesis I have received a lot of support and assistance. I would like to say a special thank you to my supervisor, Dr. Ahmed Saif. His guidance and insights throughout this process have been instrumental to formulating the methodology. I would like to acknowledge Dr. Noreen Kamal and Dr. Jong Kim, your expertise in health pushed me to broaden my thinking and bring my work to a higher level. In addition I would like to thank Matthew Murphy for providing invaluable feedback and knowledge about COVID-19 in Nova Scotia.

Chapter 1

Introduction

Epidemics and pandemics have become a major concern for policymakers around the world. What most people considered a distant threat turned into a catastrophic reality when the World Health Organization (WHO) declared the Coronavirus Disease 2019 (COVID-19) a pandemic in March 2020. Despite the drastic actions taken by governments, approximately 205 million COVID-19 cases and 4.3 million deaths have been reported globally as of August 2021. Given the enormous cost humanity has been paying due to COVID-19, experts warn that the world cannot afford to be unprepared again when the next pandemic hits (15).

1.1 Existing Research

It is possible to reduce the spread of an epidemic disease caused by a respiratory virus such as COVID-19 through measures that involve minimizing people's contact, which can be achieved by implementing policies that, for example, restrict travel and ban gatherings. These policies, however, have substantial economic and societal costs if implemented for extended periods. Thus, selecting from the wide array of response policy alternatives to minimize the health impacts of an epidemic without causing disastrous side effects on the economy and the health of people, including mental health and delayed surgeries, is a challenging task for policymakers. In the absence of systematic and evidence-based methods to develop response strategies, policymakers have no choice but to rely on ad-hoc and reactive responses, which might be far from optimum. Operations Research (OR) methods can be helpful in informing high quality response strategies that balance health, economic, and societal considerations. However, they are yet to be used to their full potential.

Currently, most of the quantitative methods used by practitioners to test response policies and predict the trajectory of epidemics are based on simulation models that

approximate dynamic epidemiological models like the famous susceptible-infected-recovered (SIR) model. These compartmental models are popular among practitioners due to their simplicity and intuitiveness. Other statistical (e.g., network (7)) and simulation (e.g., agent-based (45)) models have been proposed in the literature for the same purpose. While simulation models can be used for decision making by changing input parameters and observing the change in outputs, they have well-known limitations (41). When the number of possible alternatives is very large (as in the case when different policies could be implemented at different stages), simulation techniques can be used to evaluate and compare only a small subset of these alternatives. More importantly, these alternatives are restricted by the imagination of the model user. This issue is particularly vital when dealing with new situations like COVID-19. Another common issue of simulation models is the difficulty of translating their outputs into useful decisions, as the model provides a range of possible outputs for each set of parameters and inputs. There is often a significant overlap between output ranges of different strategies, rendering them of little value in policy formulation.

1.2 Thesis Contributions and Areas for Future Work

This thesis proposes a novel framework for using OR tools to devise response strategies to epidemics. This framework is a simulation-optimization that combines a compartmental model with two meta-heuristic optimization procedures to find near-optimal strategies that minimizes the number of cumulative infections given a limit on the total economic cost of the response strategy. In particular, a simulation model based on a modified, age-stratified susceptible-exposed-infected-recovered (SEIR) compartmental model is used to evaluate response strategies, each of which defines closure, protection, and travel policies in every time period of the planning horizon. The epidemiological model captures, in detail, the contact frequencies among different age groups, the presence of co-morbidities, and the self quarantine behaviour, among other realistic considerations. In the time-based framework, the simulation model is embedded in a Genetic Algorithm (GA) that uses the population of evaluated strategies to iteratively generate new (and hopefully better) ones through cross over and mutation. In the state-based framework, the simulation model is embedded in a Simulated Annealing (SA) algorithm that evaluates neighbor strategies to find new

and potentially better solutions. The second framework uses the same modified, age-stratified SEIR simulation model to capture the health impact of policy thresholds that determine whether restrictions should be increased, decreased, or maintained.

The research presented here was developed while working on a project with Nova Scotia Health Authority (NSHA) to build decision support tools based on OR methods that could be used by NSHA to extract response strategies to COVID-19 that strike a balance between health and economic objectives. Hence, the proposed frameworks were applied to the Canadian province of NS as a real life case study. The simulation-optimization frameworks give policymakers optimal strategies; however, the simulation (compartmental) model can also be used on its own to test strategies of interest to policymakers. The simulation model was used to test specific strategies such as immediately removing all restrictions, maintaining all restrictions, and several in between. The resulting cumulative infections, active infections, hospitalizations, and deaths from each scenario were then compared. The model used in the scenario testing was extended to include the proposed immunization plan for NS. The immunization plan was made up of multiple phases. The first two phases focused on vaccinating high risk individuals in long term care facilities and frontline workers, whereas the final phase was open to all Nova Scotians starting with people over the age of 80 and working downward in 5 year increments. All eligible and willing Nova Scotians were able to get their first dose by June 31, 2021 and the second dose a maximum of 4 months later.

Although the simulation-optimization frameworks were developed for COVID-19 in NS, they are quite generic and can be easily tailored to be used by other jurisdictions and for other epidemics. The population demographics can be modified by updating the number of individuals in each age group as well as their health status. The simulation model could be replaced by a model that considers spatial aspects, or the current compartmental model could be modified to include several connected populations. The optimization algorithms can also be modified, such as changing the single-start SA to a multi-start SA. The vaccination compartment added for the strategy testing could be added to the compartmental model used in the optimization frameworks. As well, the vaccination plan could be updated to reflect the vaccination data as the original plan was conservatively estimated.

Throughout this thesis, the term policy is used to refer to a pre-defined set of decisions specific to a single response aspect (i.e., closure, protection, or travel) in a single time period. An example is restricting all international travel during a given week. The time-based optimization framework uses the term strategy to refer to a series of policy tuples for the entire planning horizon, where each tuple consists of a closure, protection, and travel policy. The state-based optimization framework uses policy levels, where a policy level is a combination of closure, protection, and travel interventions of varying strictness. A strategy in this framework is the set of upper and lower limits that trigger a shift between different policies. There are 5 upper limits and 5 lower limits, where an upper limit means that the policy level shifts upward to a more strict level, and a lower limit means that the policy level shifts downward to a more relaxed level. A threshold is defined as the cumulative number of cases in a single time period and could represent an upper limit or lower limit for moving between policy levels.

This thesis is organized as follows: Chapter 2 reviews related work, highlighting the research gaps and the contributions of this thesis. Chapter 3 describes the simulation model components, the types of response policies considered, the mathematical formulation and how the model was verified and validated. Section 4 describes the GA used to optimize the time-based response strategies, the SA used to optimize the state-based response strategies, the numerical results obtained by implementing the proposed frameworks on the case study of NS, and provides some managerial insights. Chapter 5 describes the selected opening scenarios during vaccination, their resulting health implications, and the interpretation of findings for policymakers. Finally, conclusions and possible extensions are provided in Chapter 6.

Chapter 2

Related Work

Before describing the simulation-optimization framework proposed to optimize response strategies to COVID-19, related work is reviewed. The first part surveys the OR methods proposed in the literature to formulate response strategies to epidemics and contrasts this work with them, highlighting research gaps and contributions. This review focuses on prescriptive, as opposed to descriptive or predictive, approaches, i.e., those which aim at informing (near-)optimal response strategies, especially when a large number of strategies could be efficiently evaluated and compared. This choice, to a great extent, excludes most simulation and statistical models commonly used in the quantitative epidemiology literature, which usually have predictive or analytical purposes. Readers interested in the classical epidemiological models are referred to the texts of Brauer (4) and Kramer (26). The second part focuses on the COVID-19 pandemic, particularly the models proposed in the literature to evaluate its impact and aid policymakers in making decisions regarding public health interventions, and how they relate to this work. Given the sheer number of mathematical models developed for COVID-19, it is not possible to include all of them here. Interested readers are referred to the survey of Adiga et al. (1) for a detailed account.

2.1 The Role of OR Methods in Developing Epidemic Response Strategies

Health care has been one of the main application areas, and a prominent success story, of OR in the last four decades (40; 23; 63). However, except for widely used simulation frameworks (system dynamics (60), discrete event (32), agent-based (45)) to model the progression of epidemics, using OR tools to devise response strategies to disease outbreaks has not received much attention prior to the COVID-19 pandemic. Among the few early attempts is the work of Lee and Pierskalla (29), which

developed a mathematical program for computing the optimal test choice and screening periods in diseases which have zero or negligible latent periods. Dimitrov et al. (9) presented a tactical optimization model for distributing a stockpile of a pH1N1 antiviral treatment, which efficiently searches large sets of intervention strategies applied to a stochastic network model of pandemic influenza transmission within and among U.S. cities. Other vaccine allocation optimization approaches proposed include stochastic programming (53; 62), derivative free optimization (8) and heuristics (54). Long and Brandeau (31) surveyed the application of different OR tools, including Decision Trees, Markov Models, Network Models and Linear Programming to analyze infectious disease control decisions. One of the most related studies to this work is the simulation-optimization framework presented by Uribe-Sanchez et al. (57) to optimize mitigation strategies for pandemics affecting several regions. It allocates a limited budget to procure vaccines and antivirals, capacities for their administration, and resources required to enforce social distancing. However, two major differences between this work and the work completed by Uribe-Sanchez et al. (57) are noted. First, in their framework, available budget is allocated progressively, i.e., allocation of available resources, including remaining resources from previous allocation, is performed individually for each new regional outbreak episode (epoch), as opposed to the holistic approach used in this research to optimize the response strategy for the entire planning horizon. Secondly, and more importantly, they select non-pharmaceutical policies (e.g., social distancing, quarantine, closure) based on static guidelines that depend on pandemic severity, in contrast to this framework that lets the optimization procedure freely decide these policies for each time period.

The emergence of COVID-19 has led to a surge in its research among the OR community. OR tools have been implemented mainly to allocate resources optimally. Risanger et al. (43) presented a facility location model to determine which pharmacies in the U.S. should be testing for COVID-19 to maximize accessibility. Mehrotra et al. (34) developed a stochastic optimization model to share ventilators across the US, aiming to minimize shortfall. More related to this work, Kaplan (24) used probability models to assess the effectiveness of case isolation of infected individuals and quarantine of exposed individuals, and found that case isolation alone is sufficient to end community outbreaks, provided that cases are detected efficiently. Rawson

et al. (42) applied an optimal control framework to a modified SEIR model to investigate the efficacy of two potential lockdown release strategies. A gradual release strategy is optimized to determine how to maximize those working while preventing the health service from being overwhelmed. Although having some similarity with the proposed framework, there is a much narrower focus on releasing a locked down population and using a simple search heuristic to identify the optimal solution. Bertsimas et al. (2) address the problem of allocating vaccine quantities among geographical areas and population groups. The problem was formulated as a bilinear, non-convex optimization model and a coordinate descent algorithm that iterates between optimizing vaccine allocations and simulating the dynamics of the pandemic (using an extended version of an epidemiological prediction model known as "DELPHI") was proposed to solve it. The "DELPHI" model is an extended compartmental model adapted for COVID-19 to include under-detected cases, government and societal responses, and declining mortality rates. Similar to Bertsimas et al. (2), this research uses a simulation-optimization framework that combines an epidemiological prediction model with a search algorithm. However, this work uses GA and SA metaheuristics to effectively cover a vast search space and has a different focus on closure, protection, and travel policies rather than vaccination plans.

This review reveals that, with the exception of few noticeable attempts, OR is yet to be utilized to its full potential to guide response strategies to epidemics and pandemics. It is argued that OR methods and tools can play an important role in informing high-quality policy alternatives that formally model policymakers' objectives, restrictions, and priorities, as opposed to the widely used trial-and-error methods. The framework proposed in this thesis is a significant step towards normalizing the use of OR methods in the area of response strategies to epidemic outbreaks. From the completed literature review, this is the first comprehensive OR-based framework for optimizing a multifaceted (i.e., closure, protection, travel) pandemic response strategy over a long-time horizon while trying to strike a balance between health and economic considerations. This framework has a broader scope and higher flexibility than previous studies. Unlike the simple models used in some past studies, the detailed epidemic model used in this study adequately captures the characteristics and behaviours of the population (e.g., age groups, co-morbidities, contact patterns,

quarantine, infection severity, hospital, and intensive care unit (ICU) admission, introduction of new cases through travel). Furthermore, using metaheuristics like GA and SA enables the exploration of the vast search space and reach (near-)optimal strategies effectively, as opposed to the simple heuristics proposed in the literature.

2.2 COVID-19 Models and Response Policies

COVID-19 is a respiratory illness caused by a novel type of the coronavirus called Severe Acute Respiratory Syndrome Coronavirus 2 (SARS-CoV-2), which has proven to be a dangerous pathogen due to its high infectivity, long incubation period, and acute health impact on the population. Compartmental models have been used extensively to study the spread of the virus and to evaluate potential intervention policies. Among them, modified SEIR models were the most widely used since they were deemed more suitable to capture the disease profile. Two representative examples for COVID-19 are Tuite et al. (56) and Giordano et al. (14) which utilized modified SEIR models, though with different additional compartments, to evaluate interventions such as case identification or contact tracing, case isolation, and social distancing. Both reached the same conclusion, that contact tracing and isolation on their own are insufficient to prevent the epidemic spread and that social distancing measures are necessary to prevent over-burdening of the health system. Tuite et al. (56) also compared fixed versus dynamic strategies and showed that dynamic strategies have a comparable effectiveness in maintaining cases below ICU capacity but result in less overall time under restrictive policies. However, neither of the models offered precise policy prescriptions in terms of how the reductions associated with physical distancing strategies that were modeled are to be achieved. Another limitation was that policymakers must have the strategy determined beforehand to test.

A few models in the literature attempted to evaluate and devise response strategies while considering the opposing goals of reducing infections and the economic and health burdens simultaneously. Toda (55) used two separate models, an SIR compartmental model, and a stylized production-based asset pricing model, respectively, to evaluate the disease spread and economic impact. An optimal policy introducing social distancing depending on the average number of cases was determined and showed a reduction of 21.8 % in peak cases. The economic model used to evaluate

the intervention policy showed that while it leads to two disease peaks, its expected economic decline is moderate, amounting to 10% only compared to 50% for the single peak base case. Guadalupe (58) also used an SIR model while measuring economic impact by looking at the time to reach steady state for different quarantine strategies. It is assumed that the faster a policy results in reaching steady state it will have a lower impact on the economy. Both models have the same limitation seen above where they do not offer detailed strategies on when to implement interventions and for how long. Popa (39) proposed a combinatorial optimization model to optimize social distancing policies while taking into consideration their impact on the economy. For a given total budget, the model determines its optimal allocation between isolating people and closing facilities. Hence, it requires a significant amount of granular data e.g., all facilities and the associated cost of closing them, as well as people and their associated cost of isolating, making it difficult to test and validate. Other models that evaluated case management strategies included: a system of integro-differential equations (25) and dynamic transmission models based on the Erlang and Poisson distributions (64). The models used similar interventions including lockdowns, social distancing, and contact tracing. They also had similar results stating the importance of using all interventions concurrently to ensure that health systems are not overwhelmed by cases. Furthermore, it is shown that early lockdown without additional public health interventions will result in a delayed second wave of similar magnitude once restrictions are lifted.

As COVID-19 remains to be a major threat, new models are being developed to offer insights into managing it from a policy perspective. However, a notable gap with the current models is that, while they show that public health interventions are needed to manage COVID-19 cases, they do not offer precise prescriptions that inform policymakers what level of intervention to implement and when. Moreover, these models, regardless of their accuracy and sophistication, can evaluate only the strategies predetermined by the policymaker, but not develop new ones. This research fills these gaps by developing a systematic approach that enables detailed and dynamic response strategies to be generated and evaluated efficiently, thus helping policymakers to make informed decisions.

2.3 Research Aim and Objectives

The gaps highlighted in the previous section give rise to the aims and objectives of this research. The aim of the research is to develop prescriptive decision support tools for policymakers to devise optimal policy strategies to minimize the impacts of infectious disease spread. These tools should be capable of being adapted to various diseases or locations with the adjustment of model parameters. The objectives include:

1. Develop a compartmental model to accurately depict the transmission and health impact of COVID-19 in NS
2. Construct a simulation-optimization framework that uses the compartmental model along side an optimization algorithm to derive optimal response strategies to minimize the economic and health burden
3. Test opening scenarios in NS of varying strictness

Each of these objectives is addressed in one of the following three chapters: SEIR Compartmental Model (3), Simulation-Optimization Approach (4), and Scenario Testing (5).

Chapter 3

SEIR Compartmental Model

In this section, the central component of the decision support tools is presented, which is a modified, age-stratified SEIR model that evaluates the health impact (i.e., total number of infections) of response strategies. This section begins by outlining the model structure, then describing the response policies considered, presenting the mathematical formulation, and finally showing how the model is verified and validated.

The SEIR model is a compartmental model in which the population is divided into compartments and people move between compartments at different rates of transfer (4). It is an expanded version of the famous Kermack-McKendrick' SIR model (27) with an exposed compartment added. The susceptible (S) compartment contains people who are able to contract the disease. The exposed (E) compartment has people who have been infected but are not yet infectious. The infected (I) compartment consists of people who are infectious and capable of spreading the disease. The recovered (R) compartment contains people who have been infected and either have immunity or died, meaning they can no longer get the disease and spread it to others. The independent variable in the model is time, and the rate of transfer between compartments is described mathematically using differential equations. Figure 3.1 shows a flowchart representation of the SEIR model, highlighting the different compartments and the flows between them. This flowchart is based on the model structure developed in Tuite et al. (56). A stock-and-flow diagram of the same model (constructed using *Vensim*) is shown in Figure 3.2. The model begins with the susceptible compartment which encompasses the population under study. Susceptible can lead into two categories: exposed, which refers to people who have been exposed to the disease and are continuing to move around the community, and exposed (quarantined), which refers to people who have been exposed to the disease but have been identified

through contact tracing and are self-isolating according to restrictions. The two exposed streams transition into the pre-symptomatic infection period where individuals can spread the disease but do not have symptoms yet. The infection period follows the pre-symptomatic period and is classified by mild-moderate or severe. The separation of infection into two categories is because individuals have different likelihood of outcomes depending on the disease severity. When an individual moves into the severe compartment it does not mean they go from no symptoms to severe symptoms. It means the individual will develop into a severe case, whether initially they have mild to moderate symptoms or start with severe symptoms. The mild-moderate compartment and a portion of the severe compartment will recover, while the remaining severe cases will move into the hospitalization compartment. From the hospital, patients can recover or move into the intensive care unit (ICU). Those patients in the ICU can then recover or die.

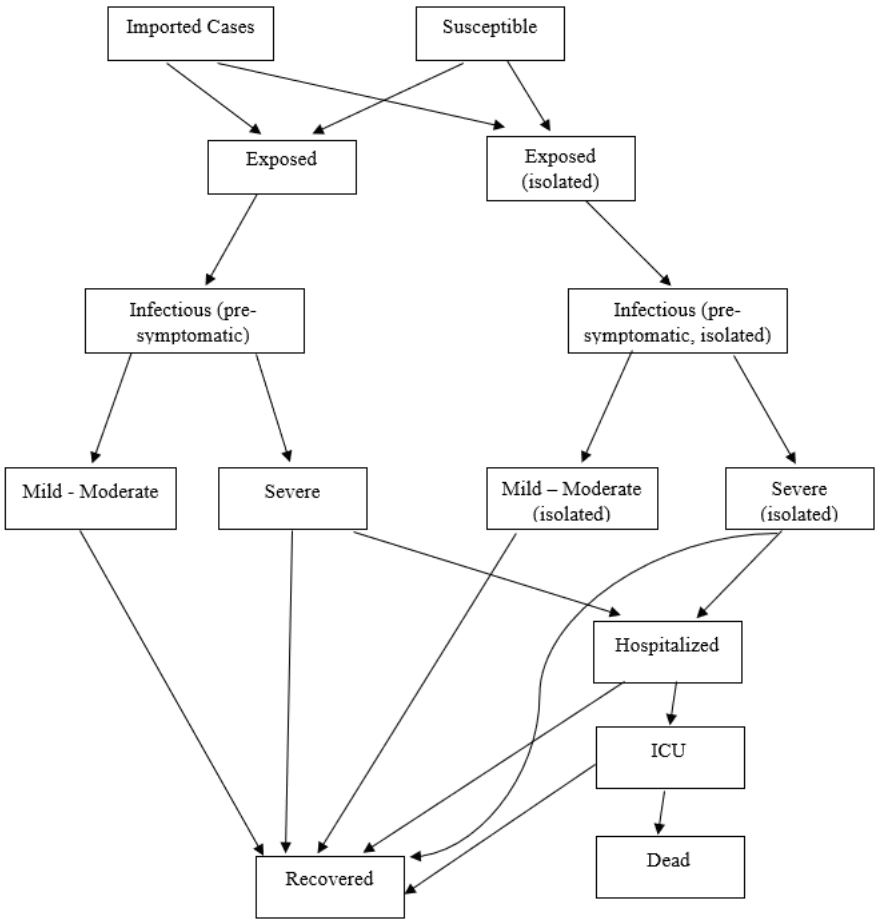

Figure 3.1: Flow diagram of disease compartments used in the modified SEIR model

Like most compartmental models, the SEIR model is built on basic assumptions, including that the epidemic process is deterministic and that the number of members in a compartment is a differentiable function of time, which only becomes accurate once there are significant number of infections. It is also assumed that the time scale of the disease is much faster than births and natural deaths, so demographic effects are ignored. Furthermore, the following assumptions are made in the SEIR model:

1. No re-infection is possible and recovered individuals remain immune;
2. The model runs in periods of one week, meaning that a policy change can occur at a maximum of once per week;
3. An individual is only infectious during the pre-symptomatic, mild-moderate, and severe compartments;
4. Individuals have the same duration in a compartment regardless of age or health status; and
5. The model is a closed system and the population is constant.

The model is based on the case study of COVID-19 in NS and all inputs are modified to accurately depict it. These inputs include population demographics and health status.

3.1 Model Parameters

The age distribution of the NS population was incorporated by stratifying by age, and each group was further stratified by health status. There are seventeen age groups in 5-year increments using 2019 population data from Statistics Canada (48). The health status stratification comprises of two categories: those with and those without comorbidities. A comorbidity is an underlying health condition or disease that is present within an individual. Examples of common comorbidities include: heart disease, asthma, diabetes, stroke, and cancer. It is important to understand the health characteristics of the population, as it has been found that underlying conditions can have a significant impact on patient outcomes (61; 59). Statistics Canada released population health data outlining the percentage of the population by age category

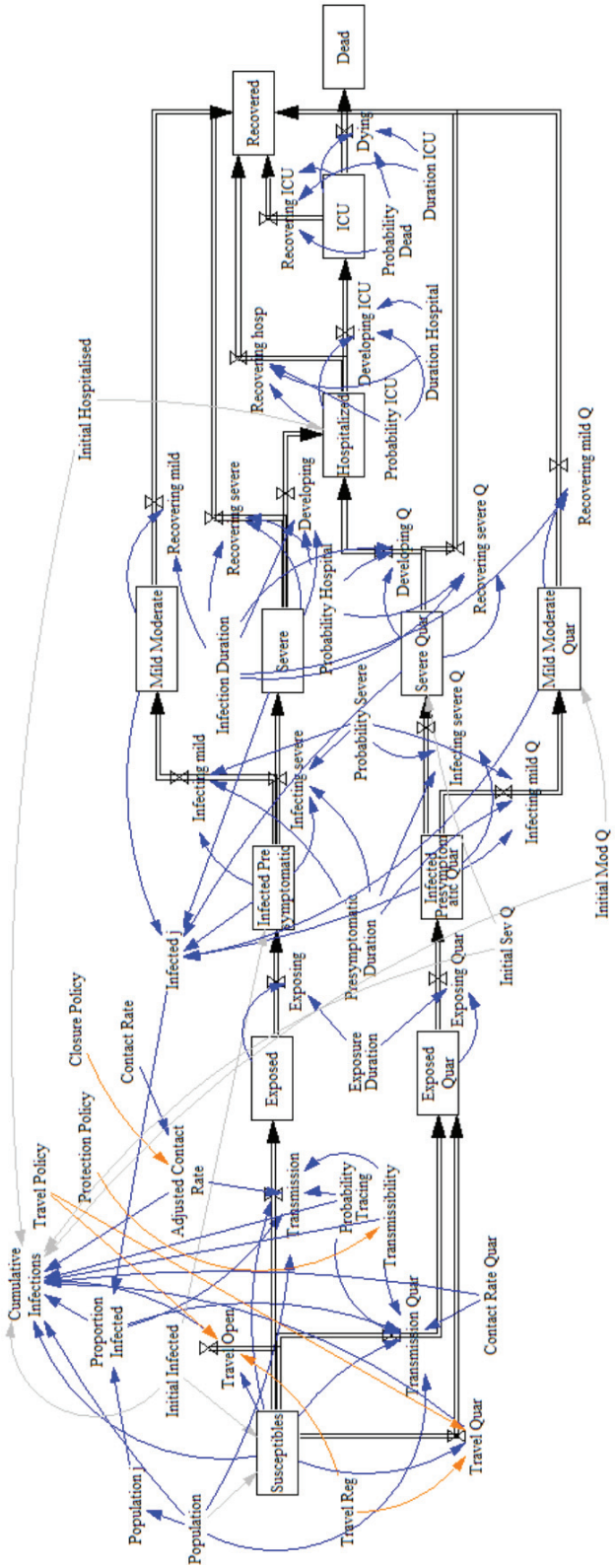

Figure 3.2: Detailed stock and flow diagram developed in Vensim

with at least one underlying health condition that will increase the likelihood of a severe outcome given infection with COVID-19 (47). This data only pertained to Canadians over age 18, thus, to account for increased severity in Canadians under 18, Asthma data was used (16). It was assumed this would be sufficient as the majority of younger people do not have diseases such as hypertension or stroke. The parameters describing the clinical course of COVID-19 were derived from Tuite et al. (56) and can be seen in Table 3.1.

Due to the evolving nature of COVID-19 there is limited data about the disease parameters, transmission dynamics, and impacts of policy restrictions. There is a wide variety of publications and research which resulted in a large range of estimates used for modelling. For example, Tuite et al. (56) estimated the latent period to be 2.5 days in their model whereas Giordano et al. (14) used a latent period of 0 days. As the knowledge and body of research surrounding COVID-19 increases it can be noted that parameters such as basic reproduction number or patient outcomes, like death, change based on the population demographics, COVID-19 variant under study, and social norms within a region. Gallo et al. (13) completed a rapid review of literature to identify and quantify epidemiological parameters that impact COVID-19 transmission. The review's key findings were that the basic reproduction varied between 0.48 and 14.8, and was very sensitive to local context. The median hospitalization time also had significant variation, between 1 and 3 weeks. In this thesis, the variation in data was dealt with by choosing reliable sources and reviewing parameters with NSHA experts to verify they were inline with what was being observed within NS.

3.1.1 Contact Tracing

Contact tracing is a public health intervention used to control the spread of COVID-19. It is the process of identifying, assessing, and managing individuals who have been exposed to COVID-19 to prevent further transmission. In NS, once an individual is contacted, there are three potential action plans depending on their risk level (36). The action plans have changed throughout the pandemic for each risk level: low, moderate, and high. As of February 2021, a low risk classification does not require any action, but it is recommended they complete a phone assessment. A moderate risk must take a COVID-19 test and self-isolate while waiting for the results. If the test

Table 3.1: Model parameters

Parameter	Age Group	Health Status	Value	Description	Source
Contact Tracing	All	All	0.3	Proportion of contacts notified of exposure	NSHA
Exposure Duration	All	All	2.5	Average time an individual is infected prior to onset of infectiousness (days)	(56)
Pre-symptomatic Duration	All	All	1	Average time an individual is infectious prior to onset of symptoms (days)	(56)
Infection Duration	All	All	6	Average time an individual is infectious and symptomatic (days)	(56)
Hospital Duration	All	All	10	Average time an individual is hospitalized (days)	(56)
ICU Duration	All	All	21	Average time an individual is in intensive care (days)	(56)
Probability Severe Infection				Likelihood a severe infection develops	(56)
	<15	No Comorbidities	0.01		
	15-49	No Comorbidities	0.03		
	50-69	No Comorbidities	0.12		
	70+	No Comorbidities	0.35		
	<15	Comorbidities	0.02		
	15-49	Comorbidities	0.06		
	50-69	Comorbidities	0.25		
	70+	Comorbidities	0.76		
Probability Hospitalisation				Likelihood of hospitalisation	(56)
	<20	No Comorbidities	0.011		
	20-29	No Comorbidities	0.021		
	30-39	No Comorbidities	0.025		
	40-49	No Comorbidities	0.035		
	50-59	No Comorbidities	0.077		
	60-79	No Comorbidities	0.159		
	70+	No Comorbidities	0.262		
	<20	Comorbidities	0.024		
	20-29	Comorbidities	0.044		
	30-39	Comorbidities	0.054		
	40-49	Comorbidities	0.075		
	50-59	Comorbidities	0.165		
	60-79	Comorbidities	0.34		
	70+	Comorbidities	0.561		
Probability ICU	All	All	0.26	Likelihood intensive care is needed	(56)
Probability Death				Likelihood of dying	(56)
	<15	No Comorbidities	0		
	15-49	No Comorbidities	0.2		
	50-69	No Comorbidities	0.36		
	70+	No Comorbidities	0.58		
	<15	Comorbidities	0		
	15-49	Comorbidities	0.53		
	50-69	Comorbidities	0.9		
	70+	Comorbidities	1		

comes back negative, self-isolation is no longer required. A high risk must self-isolate for 14 days, record their temperature daily, and take a COVID-19 test. Regardless of the test result, the individual must isolate for the full 14 days. Contact tracing was incorporated into the model by adding a quarantine stream. All individuals identified through contact tracing will flow through the quarantine stream. In consultation with NSHA it was determined that their conservatively estimated ability to trace contacts was 30%. This means they are able to identify 30% of an infected persons contacts and inform them of the exposure.

3.1.2 Case Importation

Travel restrictions are another public health intervention that can be implemented to manage infections and the transmission of COVID-19. By restricting travel, the opportunity for introduction of new cases is limited, which minimizes the likelihood of community spread and increased cases. Travel restrictions have clear benefits when the region has few or no cases, which has been the case in NS (46). There are four different levels of travel policies in the model: No travel, Atlantic Canada travel, National travel, and International travel. For each travel policy, the estimated number of daily imported COVID-19 cases was determined. The purpose of separating domestic travel into National and Atlantic was due to the implementation of the Atlantic Bubble. The Atlantic Bubble was the agreement among Atlantic Canadian provinces that permitted free movement between them without the need for isolation (17).

Statistics Canada provides data for the number of international and domestic travellers that visited NS in 2017 and 2018 (50; 49). This data was used to estimate the number of people that visit NS from within Canada and from outside of Canada, respectively. A simplifying assumption was made that the travellers are evenly distributed throughout the year. The yearly estimate was used to determine the number of incoming travellers per day. The international travel data from Statistics Canada reported the top 13 countries international travellers originate from. The prevalence of COVID-19 was then estimated in cases per million for each country (44). Bhatia and Klausner (3) determined the probability that a random community contact has COVID-19 in the United States. A ratio of cases per million between the United States and the remaining 12 countries was used to determine the probability of a random

traveller having COVID-19 for each country. The international travellers originating from the United States accounted for approximately 4/5 of all travellers with the remaining 1/5 spread between the remaining countries. Therefore, a weighted average probability for an international traveller was determined, with the United States accounting for 78.05% and an average of the other countries for the other 21.95%. The weighted average probability of a traveller having COVID-19 is dependent on the country of origin in combination with the quantity of daily travellers, allowing for the calculation of the number of daily incoming travellers with COVID-19.

In the model, the imported cases were defined in terms of the subscripts: age group and health status. Statistics Canada describes the age distribution of people that travel domestically in Canada. It was assumed that incoming international travellers would have a similar age distribution. This data was then applied to each case importation rate, including international, to determine the distribution of incoming COVID-19 cases. The incoming travellers need to be assigned a health status in the model, it was assumed that travellers would be healthy and therefore have no-comorbidities. While this may not be realistic, the number of imported cases is relatively small in comparison to the size of the NS population, so it should have little impact on the results. When cases are imported, they come directly from the existing susceptible population and move into the exposed compartments because the model assumes a closed population. It is assumed that infected travellers will interact with the NS population and cause new infections.

3.1.3 Transmission

While transmission occurs during some form of contact between individuals, contact with an infected individual does not guarantee transmission of infection. The transmission rate is a combination of the contact rate and the probability of transmission upon contact (27). In this thesis, the probability of transmission upon contact is referred to as transmissibility. The probability is dependent on several factors including the closeness and duration of the contact, infectivity of the disease, and susceptibility of the individual. Transmissibility can be impacted by public health interventions such as social distancing, which reduces the likelihood of transmitting the disease by increasing the distance between individuals. The transmissibility value given no

interventions used for this research was 15.6% (38). This value was taken from a study in Phuket, Thailand that recorded the percentage of high risk contacts of infected individuals that had developed COVID-19. A high risk contact was defined as a contact who spent longer than five minutes exposed to a confirmed case without a facial mask or being within physical distance of one meter. The simulation model includes two public health interventions that impact disease transmissibility: masks and social distancing. Chu et al. (6) studied the impact of different interventions, including social distancing, wearing eye protection, or wearing masks on the reduction in transmission of respiratory diseases. A comparison group and intervention group were used to show the chance of viral infection with and without the intervention i.e. social distancing. The study found that incorporating social distancing resulted in a reduction in transmission of 10.2%, with a 95% CI of [%11.5, %7.5], and wearing masks alone resulted in a reduction of transmission of 14.3%, with a 95% CI of [%15.9, %10.7]. The authors estimate their confidence in the results, stating that the effect of social distancing has moderate certainty and wearing masks has low certainty. The low certainty in masks is partially attributed to the utilization of different mask types including: N95 or surgical. This is a limitation with the study as different mask types could potentially result in a more or less substantial reduction in transmission. The reduction in transmissibility of 10.2 points was used because of the higher certainty; therefore, the transmissibility with public health interventions in place was estimated to be 5.4%. A limitation with the data is that it is assumed that there is 100% mask and social distancing compliance, which results in a full reduction in transmissibility.

3.1.4 Contact Matrices

Transmission of COVID-19 is driven by individuals' social contacts. The definition of a social contact is taken from Mossong et al. (35) where it is defined as either skin-to-skin contact such as a kiss or handshake (a physical contact), or a two-way conversation with three or more words in the physical presence of another person but no skin-to-skin contact (a nonphysical contact). The study found that contact patterns were highly assortative with age: schoolchildren and young adults in particular tended to mix with people of the same age (35). The typical SEIR framework assumes homogeneous mixing between individuals, which does not accurately represent

population mixing dynamics. To mitigate the impact on the validity of the model, mixing between individuals was stratified by age. Mossong et al. (35) determined contact patterns for different age groups to help understand the spread of respiratory diseases. The study collected data from 8 countries: Poland, Belgium, Germany, Finland, Great Britain, Italy, The Netherlands, and Luxembourg. An average of the age-age contacts for all countries was used to determine the contact matrix with no public health interventions. The contact matrix was calibrated using the transmissibility parameter to get an acceptable basic reproduction number (R0) of 3.47 (37), where R0 represents the number of secondary infections cause by a single infected member into a completely susceptible population. Its value determines whether a disease will cause an epidemic (when $R0 > 1$) or the infection dies (when $R0 < 1$). The public health interventions selected that could impact contact rates were defined in five different combinations with varying strictness. Examples of interventions included no day care, moving public school to online platforms, moving universities to online platforms, and restricting access to long-term care facilities. The no intervention contact matrix was extrapolated into 4 new contact matrices, each of which represented the estimated effect of the interventions on daily contact rates. For example, if the intervention of no day care was in effect, the age to age contacts for individuals aged 0 to 4 were reduced to 0. As well, if universities were online the age to age contacts for individuals aged 20 to 24 were reduced to 0.

3.2 Response Policies to Epidemics

Governments and health authorities can implement different policies to contain, and hopefully eradicate, epidemic outbreaks like COVID-19. Examples include setting limits on gathering sizes, imposing travel restrictions, quarantining symptomatic and high-risk individuals, conducting contact tracing, and promoting or mandating PPE usage. Each policy has multiple levels of strictness and scopes of implementation in terms of duration, geographical boundaries, and/or target population. For instance, gathering limitations can be very mild (e.g., allowing up to 100 people to gather in one place) or very strict (a total curfew), can extend for hours or months, and cover few communities or the entire country. Each policy alternative has quantifiable effects on the spread on the disease, along with economic and social costs. In general, one

can expect that the stricter the policy is and the longer it is applied, the greater the effect it has in reducing the spread, albeit the higher it costs. A rational decision maker would try to maximize the positive spread reduction effects of the implemented policies while minimizing their costs, giving rise to a multi-objective problem. It is not easy to develop an exhaustive list of response policies that could be used during epidemic outbreaks. However, this work focuses on three overarching categories: closure, protection, and travel.

The policies used in this model were derived by reviewing the policies implemented within NS from March through July 2020 (5). This allowed for review of a large variety of policies of varying strictness. Generally speaking, policies implemented during March and April imposed strict restrictions on the population, whereas the policies from May through July gradually relaxed some restrictions. Therefore, a wide range of policies implemented in NS were observed and could be used to infer what policies would be used in the future given the state of infections within the province. Examples of these restrictions include: closing childcare facilities, stopping elective surgeries, closing personal services, and online public school. The list was consolidated into three overarching categories, closure, protection, and travel, and each category was narrowed down into policies which could be quantified and were assumed to have a significant impact. The main closure components are gathering limitations and closure of public schools, universities or colleges, daycare facilities, businesses such as restaurants and stores, and public outdoor facilities. These policies focus on reducing the average number of daily contacts of an individual. There are five different closure levels which all have different strictness ranging from keeping everything open to sheltering in place. Protection policies focus on reducing transmissibility, and account for the implementation of social distancing and masks. Two protection policy alternatives are considered: enforced and not enforced. Social distancing and masks are combined into one policy as they are commonly enforced together. However, they could be separated into two alternatives. This would allow more flexibility by not restricting the capacities of businesses to allow for social distancing, and only reducing transmissibility through the use of masks. There is also data available on their effectiveness in reducing spread as seen in Chu et al. (6), however, the results are strongly associated to the mask type, such as an N95 versus cotton, which led to

the simplification of combining social distancing with masks. The travel restriction policies account for the limitations on travellers to prevent case importation. There are four travel policies, where level one is allowing all travel including international and domestic, and level four is disallowing all travel. A summary of each policy class and their levels can be seen in Table 3.2.

The weekly economic cost was determined for each policy. The closure policy costs were determined using the reduction in Canadian Gross Domestic Product (GDP) in NS (52). The GDP in February 2020 was taken as a baseline (i.e., level 1) while the GDP in April 2020 was used for the strictest closure policy (i.e., level 5). The three policies in between were scaled based on the estimated average daily contacts. The protection policy costs were estimated based on the GDP specifically for restaurants and accommodations (52). Again, the GDP in February 2020 was taken as the baseline while the GDP in July/August was used for level two. The reasoning is that April 2020 had the most significant drop at 18%; however, as business began opening with restrictions, it increased and leveled off in July and August prior to the second wave. The travel policy costs were based on the estimated loss of tourism GDP (51). It was estimated that 20% of tourism is from international visitors while 80% is from domestic visitors (30). Combining the GDP loss and visitor estimates, a cost was determined for each level. A limitation of the approach used to estimate the cost data is that it ignores the potential interaction between the costs of different interventions. The cost for each policy alternative can be found in Table 3.2.

3.3 Model Formulation

Table 3.3 depicts the notations used to formulate the compartmental model. The model consists of the system of equations (3.1)-(3.15), which describe the flow of individuals with age group i and co-morbidity status k between the different compartments in the simulation model. The flows are later approximated using algebraic (difference) equations in the discrete time simulation model by replacing dt with Δt, where Δt is the simulation step size and was set at 0.25 days. Most equations are self explanatory, though a few clarifications are warranted. As shown in Figure 3.1, the flow from the Susceptible compartment splits into two streams depending on whether the case is discovered and isolated or not. Both streams go through the same steps

Table 3.2: Description and cost of closure, protection, and travel policy alternatives

Type	Level	Description	Cost ($)
Closure			
	1	No closures	0
	2	Mild restrictions	54,232,512
	3	Moderate restrictions	114,530,501
	4	Severe restrictions	147,530,815
	5	Shelter in place	204,807,485
Protection			
	1	No interventions	0
	2	Masks required and social distancing	7,619,073
Travel			
	1	International travel	0
	2	Domestic travel	214,795
	3	Atlantic travel	1,040,711
	4	No travel	1,073,975

and merge again in the Hospitalized and Recovered compartments. Also, all cases introduced through travel are assumed to be in the exposed phase, thus are added to the Exposed compartments (with or without quarantine, depending on the policy applied) and deducted from the Susceptible compartment to keep the total population unchanged. It is clear that the flows are dependent on selection of the closure, protection, and travel policies.

Table 3.3: Model notations

Indices	
i, j	Age group, $i, j = 1, \ldots, J$
k	Co-morbidity status, $k = 1, \ldots, K$
t	Time period, $t = 1, \ldots, T$
l	Closure policy, $l = 1, \ldots, L$
p	Protection policy, $p = 1, \ldots, P$
q	Travel policy, $q = 1, \ldots, Q$
Parameters	
$n_{i,k}$	Population of age group i with co-morbidity status k
$c_{i,j,l}$	Contact rate for a person in age group i with people in age group j under closure policy l
$cq_{i,j}$	Contact rate for a quarantined person in age group i with people in age group j
α_1	Average exposure duration
α_2	Average pre-symptomatic duration
α_3	Average infection duration
α_4	Average hospital duration
α_5	Average ICU duration
σ^t	Proportion contacts traced
$\sigma^s_{i,k}$	Probability of severe infected, given infected
$\sigma^h_{i,k}$	Probability hospitalized, given severe infected
σ^c	Probability ICU, given hospitalized
$\sigma^d_{i,k}$	Probability death, given ICU
τ_q	Rate of new exposed cases introduced by travel policy q
λ_i	force of infection
λ_{q_i}	quarantine force of infection
γ_p	Transmissibility under protection policy p
Compartments	
$S_{i,k}$	Number of susceptible of age group i with co-morbidity status k
$E_{i,k}$	Number of exposed of age group i with co-morbidity status k
$IP_{i,k}$	Number of infected pre-symptomatic of age group i with co-morbidity status k
$IM_{i,k}$	Number of infected mild-moderate of age group i with co-morbidity status k
$IS_{i,k}$	Number of infected severe of age group i with co-morbidity status k
$EQ_{i,k}$	Number of exposed quarantined of age group i with co-morbidity status k
$IPQ_{i,k}$	Number of infected pre-symptomatic quarantined of age group i with co-morbidity status k
$IMQ_{i,k}$	Number of infected mild-moderate quarantined of age group i with co-morbidity status k
$ISQ_{i,k}$	Number of infected severe quarantined of age group i with co-morbidity status k
$H_{i,k}$	Number of hospitalized of age group i with co-morbidity status k
$I_{i,k}$	Number of ICU of age group i with co-morbidity status k
$R_{i,k}$	Number of recovered of age group i with co-morbidity status k
$D_{i,k}$	Number of dead of age group i with co-morbidity status k

$$\frac{dS_{i,k}}{dt} = -\lambda_i S_{i,k} - \lambda_{q_i} S_{i,k} - \tau_q \tag{3.1}$$

$$\frac{dE_{i,k}}{dt} = \left(1-\sigma^t\right)\lambda_i S_{i,k} + \tau_q - \left(\frac{1}{\alpha_1}\right) E_{i,k} \tag{3.2}$$

$$\frac{dIP_{i,k}}{dt} = \left(\frac{1}{\alpha_1}\right) E_{i,k} - \left(\frac{1}{\alpha_2}\right) IP_{i,k} \tag{3.3}$$

$$\frac{dIM_{i,k}}{dt} = \left(1-\sigma^s_{i,k}\right)\left(\frac{1}{\alpha_2}\right) IP_{i,k} - \left(\frac{1}{\alpha_3}\right) IM_{i,k} \tag{3.4}$$

$$\frac{dIS_{i,k}}{dt} = \left(\sigma^s_{i,k}\right)\left(\frac{1}{\alpha_2}\right) IP_{i,k} - \left(\frac{1}{\alpha_3}\right) IS_{i,k} \tag{3.5}$$

$$\frac{dEQ_{i,k}}{dt} = \left(\sigma^t\right)\lambda_{q_i} S_{i,k} + \tau_q - \left(\frac{1}{\alpha_1}\right) EQ_{i,k} \tag{3.6}$$

$$\frac{dIPQ_{i,k}}{dt} = \left(\frac{1}{\alpha_1}\right) EQ_{i,k} - \left(\frac{1}{\alpha_2}\right) IPQ_{i,k} \tag{3.7}$$

$$\frac{dIMQ_{i,k}}{dt} = \left(1-\sigma^s_{i,k}\right)\left(\frac{1}{\alpha_2}\right) IPQ_{i,k} - \left(\frac{1}{\alpha_3}\right) IMQ_{i,k} \tag{3.8}$$

$$\frac{dISQ_{i,k}}{dt} = \left(\sigma^s_{i,k}\right)\left(\frac{1}{\alpha_2}\right) IPQ_{i,k} - \left(\frac{1}{\alpha_3}\right) ISQ_{i,k} \tag{3.9}$$

$$\frac{dH_{i,k}}{dt} = \left(\sigma^h_{i,k}\right)\left(\frac{1}{\alpha_3}\right)\left(IS_{i,k} + ISQ_{i,k}\right) - \left(\frac{1}{\alpha_4}\right) H_{i,k} \tag{3.10}$$

$$\frac{dI_{i,k}}{dt} = \left(\sigma^c\right)\left(\frac{1}{\alpha_4}\right) H_{i,k} - \left(\frac{1}{\alpha_5}\right) I_{i,k} \tag{3.11}$$

$$\frac{dD_{i,k}}{dt} = \left(\sigma^d_{i,k}\right)\left(\frac{1}{\alpha_5}\right) I_{i,k} \tag{3.12}$$

$$\begin{aligned}\frac{dR_{i,k}}{dt} = {} & \left(\frac{1}{\alpha_3}\right)\left(IM_{i,k} + IMQ_{i,k}\right) + \left(1-\sigma^h_{i,k}\right)\left(\frac{1}{\alpha_3}\right)\left(IS_{i,k} + ISQ_{i,k}\right) + \left(1-\sigma^c\right)\left(\frac{1}{\alpha_4}\right) H_{i,k} \\ & + \left(1-\sigma^d_{i,k}\right)\left(\frac{1}{\alpha_5}\right) I_{i,k}\end{aligned} \tag{3.13}$$

$$\lambda_i = \gamma_p \sum_{j=1}^{J} c_{i,j,l} \left(\frac{\sum_{k=1}^{K}\left(IP_{j,k} + IM_{j,k} + IS_{j,k}\right)}{\sum_{j=1}^{J}\sum_{k=1}^{K} n_{j,k}}\right) \tag{3.14}$$

$$\lambda_{q_i} = \gamma_p \sum_{j=1}^{J} cq_{i,j} \left(\frac{\sum_{k=1}^{K}\left(IP_{j,k} + IM_{j,k} + IS_{j,k}\right)}{\sum_{j=1}^{J}\sum_{k=1}^{K} n_{j,k}}\right) \tag{3.15}$$

3.4 Model Verification and Validation

In what follows, a brief explanation on how the compartmental model was verified and validated is provided. Verification aims to ensure that the computer programming and implementation of the conceptual model are correct. Validation, on the other hand, aims to ensure that the system accurately depicts reality.

3.4.1 Verification

Model verification was primarily performed by comparing the results obtained from three computer programs written based on the conceptual model using different platforms: an Excel spreadsheet, a Vensim stock-and-flow model (Figure 3.2), and a computer code on Julia. The Vensim model was built first in small sub-modules that were tested and debugged individually before being added up iteratively until the entire model is assembled. The equations were then written in excel to verify they were operating as intended in Vensim. The Julia code was completed last and eventually used in the simulation-optimization framework. Several instances were tested in each platform and ensured that all three models led to the same results.

3.4.2 Validation

Model validity was established by, first and foremost, determining its structure in consultation with health policy experts at NSHA and obtaining its data from highly credible sources. Moreover, a sensitivity analysis was performed to understand the uncertainty around the input parameters and their impact on cumulative infections. The parameters selected were transmissibility, contact rate, quarantine contact rate, probability tracing, exposure duration, pre-symptomatic duration, infection duration, and initial infected. To perform the analyses, some model parameters were replaced by a weighted average to allow for sampling. Two sensitivity analyses were performed: univariate and multivariate. The univariate analysis focuses on the effect of each parameter individually. The parameter values are initialized using the current value defined in Chapter 3 or a weighted average such as for contact rate. The parameters that changed depending on the subscripts such as age or comorbidity status were modified to a weighted average, as a subscripted value cannot be sampled. The simulation time was set to 100 days. During a simulation run, the model will sample from a uniform random distribution to determine a new parameter value while holding all other parameters constant. The uniform distribution limits for each parameter were $\pm$ 10% of the nominal/mean value. For example, the probability tracing parameter is initialized at 0.3, and during a run the model will sample between [0.27,0.33]. An output parameter needs to be defined and the model will monitor how the changed parameter will impact the output. The output selected was cumulative infections.

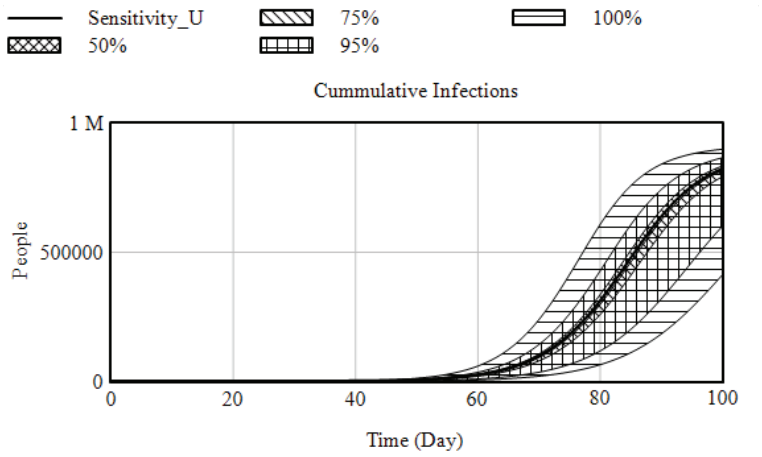

Figure 3.3: Univariate sensitivity analysis of model parameters on cumulative infections over a 100 day period

There were 200 simulation runs performed for each parameter for a total of 1600 runs. Figure 3.3 displays the results of the univariate analysis on cumulative infections over 100 days. The confidence bounds at 50%, 75%, 95%, and 100% are also included. The minimum cumulative infections, maximum cumulative infections, and range from the set of 200 simulations for each parameter are summarized in Table 3.4.

Table 3.4: Univariate sensitivity analysis results on cumulative infections by parameter over a 100 day period

Parameter	Minimum	Maximum	Range
Transmissibility	549,683	901,984	47%
Contact Rate	574,184	875,188	43%
Contact Rate Quarantine	812,042	829,335	2%
Probability Tracing	759,003	860,514	14%
Exposure Duration	784,656	847,144	8%
Pre-symptomatic Duration	802,829	836,4038	4%
Infection Duration	732,640	870,382	18%
Initial Infected	813,278	827,236	2%

The results of the univariate analysis show that changes in the transmissibility and contact rate have the most significant impact on the cumulative infections. The users of the model should take into consideration the potential inaccuracy in the model output if these values are not accurate. The parameters should also be updated as new information becomes available on the transmission of COVID-19. The remaining

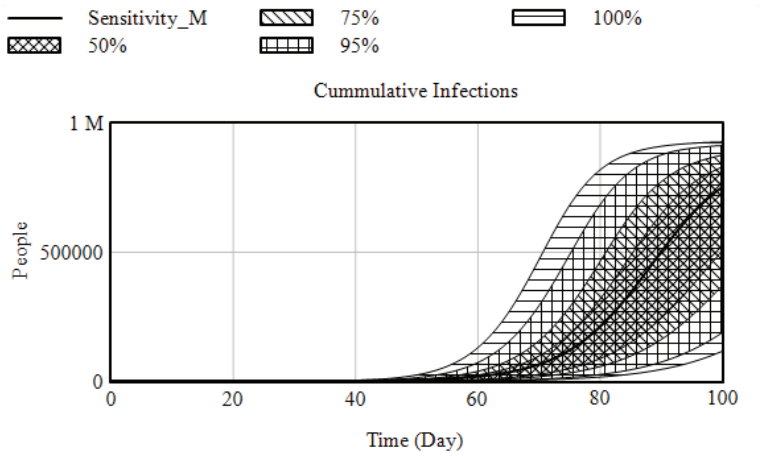

Figure 3.4: Multivariate sensitivity analysis of model parameters on cumulative infections over a 100 day period

parameters have a smaller impact on model output and therefore do not need to be scrutinized or updated to the same degree.

The multivariate analysis observes the impact of changing model parameters simultaneously. The same parameters used in the univariate analysis were used in the multivariate analysis and a simulation period of 100 days was selected. During a simulation run, the model will sample from a uniform random distribution to determine a new parameter value for all parameters. The uniform distribution limits for each parameter were ± 10% of the nominal/mean value. There were 200 simulations performed each with a different combination of parameters within the uniform random distributions. Figure 3.4 displays the results of the multivariate analysis on cumulative infections over 100 days. The confidence bounds at 50%, 75%, 95%, and 100% are also included. The multivariate analysis results show that there are interaction effects between the parameters and changing them simultaneously results in significant variation in the model output. The minimum and maximum number of infections obtained from the multivariate sensitivity analysis were 130,239 and 938,060 people, respectively.

Lastly, the model output was retrospectively compared to the initial infection wave that occurred in NS. The policies were combined and implemented following a similar timeline to what was actually enforced. The model was run for a period of 120 days starting on March 1st, 2020. The model resulted in 1070 cumulative infections with a peak daily cases of 429, while NS had 1087 cumulative infections with a daily peak of

422. Figure 3.5 shows the active cases obtained from the model and the actual active cases for NS. Although this model predicted a faster spread and an earlier peak of the epidemic, the differences in cumulative infections and daily peaks were 1.56% and 1.57% only, leading to the conclusion that the model is valid.

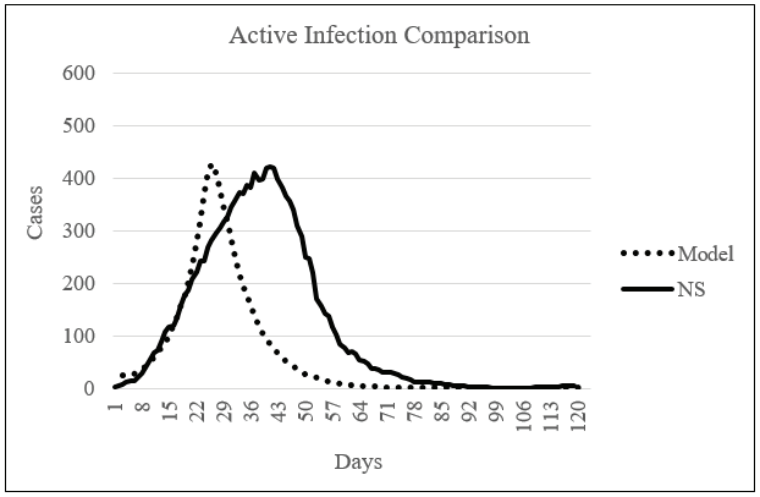

Figure 3.5: Compartmental model active infections and Nova Scotia active infections from March 2020 to June 2020

It should be highlighted that the results found in this work are based on previous parameter estimates found in literature and that the results and inferences are significantly impacted by the accuracy of the parameters. To ensure the usefulness of the results, the parameters should be updated to reflect the most accurate estimates to date.

Chapter 4

A Simulation-Optimization Approach

The compartmental model described in the previous section is embedded in two separate optimization frameworks, a time-based, which aims to find a proactive strategy, and a state-based, which aims to find a reactive one. Using a simulation-optimization framework enables a large number of response strategies to be evaluated effectively and accurately, which makes it a favorable alternative to both pure simulation (compartmental) and mathematical programming methods. While mathematical programming produces a global optimal, the compartmental model requires substantial simplification which limits the accuracy in assessing the health impact of COVID-19. Mathematical programming was attempted, however, even with simplifying the SEIR model significantly, the problem remained too large to be solved. Table 4.1 summarizes the pros and cons of each approach considered.

Table 4.1: Strengths and limitations of different methodologies considered

	Strengths	Limitations
Compartmental	High accuracy and flexibility	Few solutions tested
	Easy to use	Can not explore new strategies
Mathematical Programming	Guaranteed optimality	Simplified model
	All solutions considered	Computationally expensive
Simulation-Optimization	High accuracy and flexibility	Local optimality
	Good exploration	Difficult implementation

4.1 GA to Optimize Time-Based Response Strategies

A GA is used as the optimization procedure as it enables effective exploration of the feasible region by gradually evolving towards a superior feasible solution. The algorithm attempts to find a solution that minimizes the total number of infections, evaluated using the compartmental model, within a pre-defined budget. Each strategy (chromosome) is encoded as a matrix of size $3 \times T$, where each column is a tuple (l, p, q) of closure, protection, and travel policies. For this case study, and as presented in

Table 3.2, the values for closure, protection, and travel are as follows, $l \in [1, 2, 3, 4, 5]$, $p \in [1, 2]$, and $q \in [1, 2, 3, 4]$. The budget constraint is implemented in the GA using a penalty function that penalizes infeasible solutions by reducing their fitness values, in this case number of cumulative infections from a strategy, in proportion to the violation of the constraint. The fitness function can be seen in equation 4.1.

$$fitness = cumulative\ infections + penalty * max(0, cost - budget). \tag{4.1}$$

There were two forms of the penalty scalar considered: a static penalty and a dynamic penalty. The static penalty remains constant while running the algorithm, however, this can result in the penalty being too strong or too weak at different phases in the evolution processes. In contrast, the dynamic penalty starts off small to allow a broad range of solutions then increases during the evolution process to slowly weed out infeasible solutions. A small analysis was completed to determine values for the static penalty and the dynamic penalty, and test which would result in the best solution (minimum cumulative infections). The fixed analysis tested four penalty values and the GA was run three times for each, for which the results are found in Table 4.2. The fixed penalty of 0.00001 resulted in the lowest cumulative infections; this value was then used in the dynamic penalty analysis. While the GA runs, it records the number of iterations completed and uses the counter to change the penalty value during the algorithm's progression. The dynamic functions considered and their results can be seen in Table 4.3. The first dynamic penalty function resulted in the fewest cumulative infections and was therefore selected.

Table 4.2: Fixed penalty analysis for the time-based optimization, comparing penalty values and resulting cumulative infections

Penalty Value	Average Cumulative Infections
0.000005	275
0.000001	296
0.00005	259
0.00001	248

The GA is given a budget then runs to find an optimal response strategy. The budgets range from \$0 at no restrictions to \$10,675,026,650 at maximum restrictions throughout the 50 week planning horizon. The GA starts by generating the initial population of feasible solutions. Initially, the solution generation was random and

Table 4.3: Dynamic penalty analysis for the time-based optimization, comparing penalty functions and resulting cumulative infections

Penalty Function	Average Cumulative Infections
0.00001×counter	87
$0.00001\times \frac{counter}{2}$	103
$0.00001 \times counter^2$	112

would generate a combination of policies using a random function. This was modified because when the budget was more constrained (less than $2 billion) the algorithm had a difficult time generating a solution within the budget by using only random numbers and would run for an excessively long amount of time. The generation method was modified by determining the midpoint budget between having no restrictions and having maximum restrictions, which is $5,337,513,325. If the budget was below the midpoint then a portion of the solutions generated favoured less expensive policies, $l \in \{1, 2\}$, $p \in \{1, 2\}$, and $q \in \{1, 2\}$ while the remaining solutions were generated randomly. Conversely, if the budget exceeded the midpoint then a portion of the solutions generated favoured expensive policies, $l \in \{3, 4, 5\}$, $p \in \{1, 2\}$, and $q \in \{3, 4\}$ and the remaining solutions were generated randomly. The algorithm then selects parents from the most fit and least fit of the initial population, randomly pairs the parents into couples, and generates two children solutions per couple using uniform crossover. Then the children solutions are mutated gene by gene using a mutation rate of d. The original stopping rule was a set number of iterations without improvement in the cumulative infections from a strategy. However, after running the model for several hours, while there were a few (maximum 5) iterations without improvement, overall, the strategy continued to improve over time. This led to changing the stopping rule to the percent improvement in the new solution over the previous best solution. This enabled a good solution, approaching the optimal, to be found significantly faster. For example, the iteration stopping rule took 7 hours to reach a strategy with 61 cumulative infections and only stopped because of a timer, whereas the percent stopping rule took 1.5 hours to reach a strategy with 63 cumulative infections. The difference in solution is 3.7%, however, it resulted in a time savings of 5.5 hours. A pseudocode of the GA is provided in Table 4.4.

The parameters in the GA were optimized using parameter tuning and comparing the runtime, solution fitness, and solution feasibility at different parameter values.

Table 4.4: A pseudocode of the Genetic Algorithm

Inputs

Population size n
Number of iterations without improvement l
Number of high fitness parents selected a
Number of low fitness parents selected b
Mutation rate d

Code

Set $counter = 1$
Randomly generate initial population of size n
Evaluate the fitness of each solution in the population
While $counter < l$ **do**
  Select a parents from the 50% most fit and b parents from the 50% least fit solutions
  Randomly pair parent solutions
  Generate two children from each pair using uniform crossover
  With probability d, mutate the genes of the children
  Evaluate the fitness of the children solutions
  if max(population fitness) $\geq$ max(children fitness) **then**
    $counter = counter + 1$
  end if
  Replace the worst $(a + b)$ solutions in the population with the children solutions
end while
Return best solution

There were four parameters that were tuned: percent improvement in solution for terminating the algorithm, the initial population size, the mutation rate, and the initial solution randomness. The initial solution randomness is defined as the proportion of solutions generated randomly or generated by favouring policies based on the budget. There were 6 trials run for each parameter. This was because of the randomness in the solution generation, and allowed an average runtime, average number of infections, and average strategy cost to be determined. The trial values and results can be found in Table 4.5. The parameters that performed the best, namely trials 2, 4, 8, and 10, were combined in the final algorithm.

The problem under consideration naturally gives rise to a multi-objective optimization problem that has two conflicting objectives: minimizing the total number of infections and minimizing the economic cost of the response strategy implemented. The goal of solving such problems is usually to obtain a set of non-dominated solutions, also known as Pareto-optimal solutions, that can be presented to policy-makers (12). The well-known ϵ-constraint method is used, which transforms the multi-objective problem into a constrained single objective optimization problem by

Table 4.5: GA parameters used in parameter optimization trials and results for each trial

	Base	1	2	3	4	5	6	7	8	9	10	11
Budget (billions)	3											
Initial Population Size	100	10	50	200								
Planning Horizon (weeks)	50											
Percent Improvement Threshold	0.07				0.05	0.1	0.01					
Fit Parents	40	4	20	80								
Unfit Parents	20	2	10	40								
Children	2											
Crossover Type	Uniform											
Mutation Rate	0.01							0.1	0.001	0.05		
Initial Solution Randomness	0.5										0.2	0.8
Runtime (seconds)	1,002	30	870	1,782	2,144	308	3,214	757	1,414	758	1,272	428
Cumulative Infections	19,976	40,065	6,179	23,882	1,325	25,869	23,68	24,610	16,076	26,432	15,318	31,982
Cost (billions)	3.617	4.636	3.147	3.351	2.815	4.231	2.739	3.457	3.296	3.761	3.178	3.805

keeping one objective while turning all other objectives into constraints (11). By minimizing the cumulative infections and converting the cost objective into a constraint, an optimal solution was determined without assigning a monetary value to human life, which is not always palatable to policymakers. This technique also allows the decision-maker to set a personalized budget for policy strategies and review alternatives of different budgets. The mathematical formulation of the optimization problem is provided in equations (4.2)-(4.10).

$$\min \quad f(X_{l,t}, X_{p,t}, X_{q,t},\ t = 1, \ldots, T) \tag{4.2}$$

$$\text{s.t} \quad c_{i,j,t} = \sum_{l=1}^{L} c_{i,j,l} X_{l,t} \qquad i = 1, \ldots, I,\ j = 1, \ldots, J,\ t = 1, \ldots, T \tag{4.3}$$

$$\gamma_t = \sum_{p=1}^{P} \gamma_p X_{p,t} \qquad t = 1, \ldots, T \tag{4.4}$$

$$\tau_t = \sum_{q=1}^{Q} \tau_q X_{q,t} \qquad t = 1, \ldots, T \tag{4.5}$$

$$\sum_{l=1}^{L} X_{l,t} = 1 \qquad t = 1, \ldots, T \tag{4.6}$$

$$\sum_{p=1}^{P} X_{p,t} = 1 \qquad t = 1, \ldots, T \tag{4.7}$$

$$\sum_{q=1}^{Q} X_{q,t} = 1 \qquad t = 1, \ldots, T \tag{4.8}$$

$$\sum_{t=1}^{T} \left(\sum_{l=1}^{L} C_l X_{l,t} + \sum_{p=1}^{P} C_p X_{p,t} + \sum_{q=1}^{Q} C_q X_{q,t} \right) \leq B \tag{4.9}$$

$$X_{l,t}, X_{p,t}, X_{q,t} \in \{0, 1\} \qquad l = 1, \ldots, L,\ p = 1, \ldots, P,\ q = 1, \ldots, Q,\ t = 1, \ldots, T. \tag{4.10}$$

The binary variables $X_{l,t}, X_{p,t}$ and $X_{q,t}$, respectively, take values 1 if closure policy l, protection policy p, and travel policy q are used in week t, and 0 otherwise. The objective function $f(.)$, which counts the cumulative infections, is evaluated through the compartmental model for given values of the decision variables. Constraints (4.3)-(4.5) link the decision variables with their corresponding policy selections to obtain the compartmental model parameters $c_{i,j,t}$, γ_t and τ_t in every week. Constraints (4.6)-(4.8) stipulate that in each week, exactly one closure, protection, and travel policy level are selected. Constraint (4.9) states that the total cost of the strategy over the

entire planning horizon must not exceed the budget B, where the parameters C_l, C_p and C_q denote the cost of implementing closure policy l, protection policy p, and travel policy q, respectively, for one week. Note that this constraint is incorporated into the fitness function of the GA using a linear penalty. Finally, (4.10) is a domain constraint.

4.1.1 Results

This section presents the results obtained from implementing the proposed framework on the case study under consideration, NS. For the purpose of demonstrating the applicability of the proposed framework and to show the trade-off between health and economic considerations, the optimal response policies over a 50 week period at varying budgets are found. The strategy cost at maximum restrictions is \$10,675,026,650, while the strategy cost with no restrictions is \$0. Originally, eleven budgets were tested, incrementally decreasing from the maximum to the minimum. However, there is a large shift downward in infections when the budget increases from \$1,067,502,665 to \$2,135,005,330. This region was explored further by creating three intermediary budgets. Table 4.6 depicts the optimal strategies at all budgets and their resulting cumulative infections. Figure 4.1 shows budgets and cumulative infections plotted against each other to give the Pareto frontier. This graph visually demonstrates to policymakers the economic and health trade-off of policy strategies. It is seen that there is a sudden decrease in cumulative infections as the budget approaches \$2B, a steady linear relation between budget and infections until \$7.5B, and diminishing returns thereafter.

There were similar trends among similar budgets, so three budgets, a low cost (\$1,334,378,331), medium cost (\$3,202,507,995), and high cost (\$7,472,518,655) are compared to demonstrate the different trends. The remaining strategies are provided in Appendix A and the costs and infections can be found in Appendix B. All three strategies, with the policy decision in each time period are displayed in Figure 4.2. For each budget the first row is the closure policy, the second row is the protection policy, and the third row is the travel policy. The heat map shows strict policies as darker and gets lighter as policies are less strict. Figure 4.3 depicts the resulting cost, cumulative infections, and weekly cases for each.

Table 4.6: Incremental budgets and cumulative infections over a 50 week period

	Budget	Cumulative Infections
1	0	693705
2	1,067,502,665	636591
2.1	1,334,378,331	554338
2.2	1,601,253,998	491254
2.3	1,868,129,664	2613
3	2,135,005,330	2419
4	3,202,507,995	1290
5	4,270,010,661	748
6	5,337,513,325	476
7	6,405,015,990	256
8	7,472,518,655	70
9	8,540,021,320	71
10	9,607,523,985	66
11	10,675,026,650	59

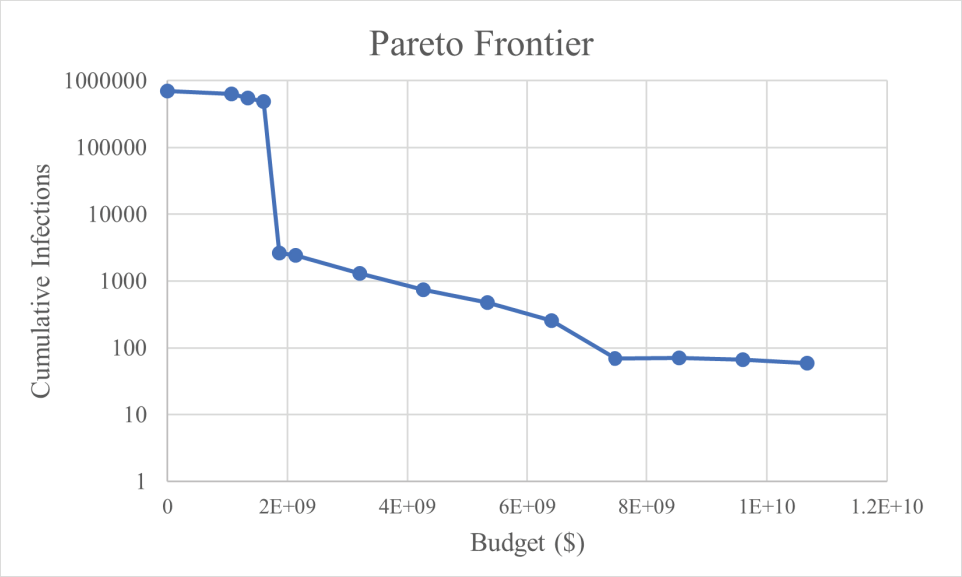

Figure 4.1: Cumulative infections plotted against cumulative strategy cost for all 14 budgets

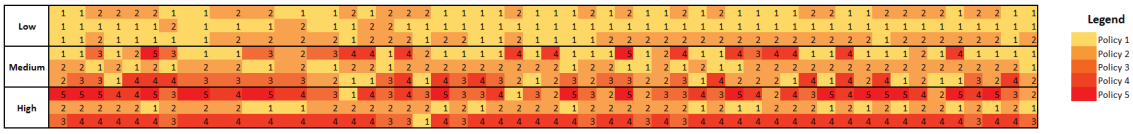

Figure 4.2: Weekly policy strategy heatmap for low, medium, and high budgets over a 50 week horizon

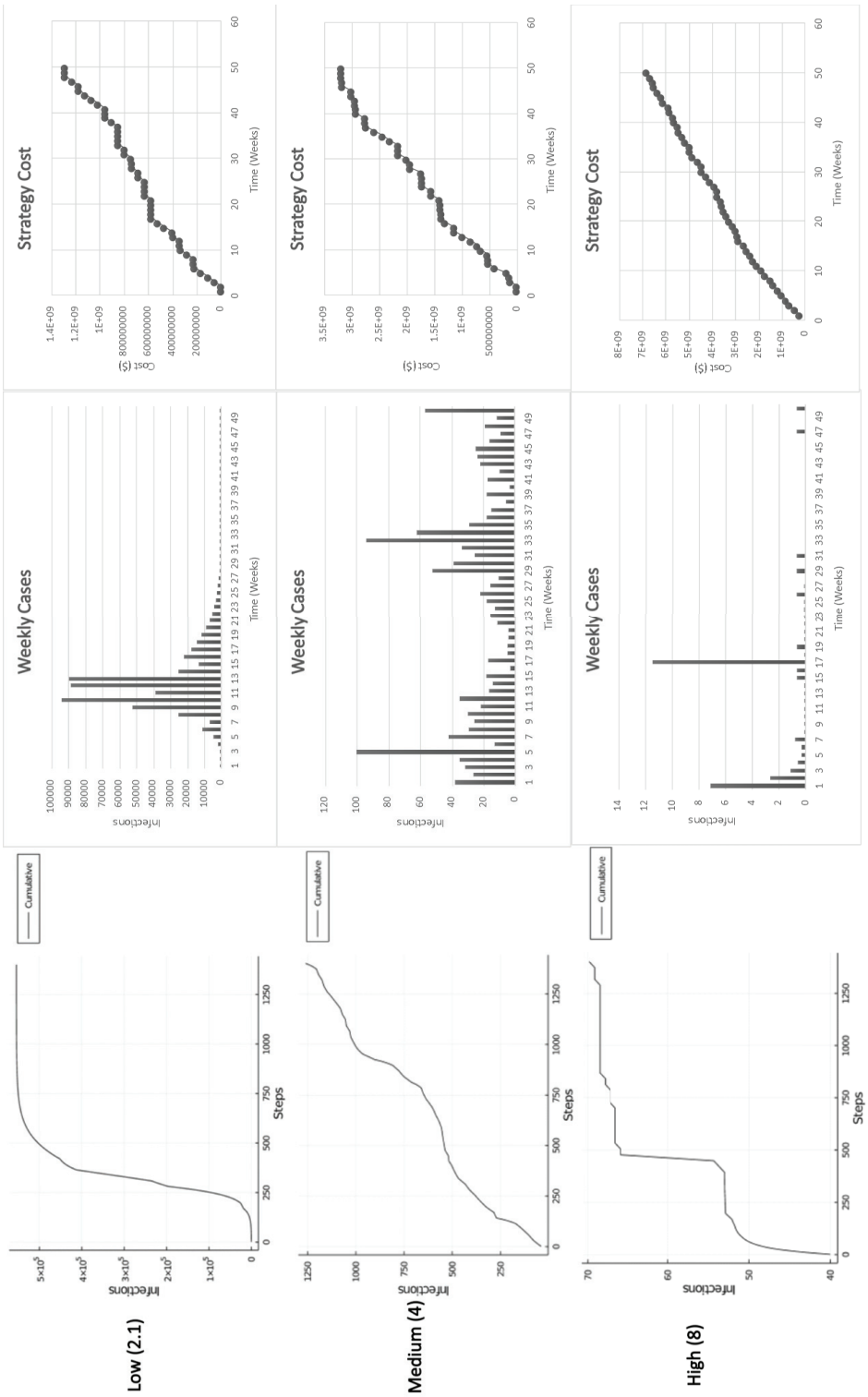

Figure 4.3: Cumulative infections, weekly infections, and cumulative strategy cost for low, medium, and high budgets over a 50 week horizon

4.1.2 Analysis

There are different trends that can be seen at the different budget levels. The higher budgets, starting at $7,472,518,655 and up, effectively place no restriction on the budget. The model chooses to impose strict policies to keep the number of cumulative infections at a very low level, all below 100. If all restrictions were at their maximum, the resulting infections is 55, therefore, once the budget approaches $7.5 billion there are diminishing returns and it is unnecessary to continue increasing the budget. Figure 4.2 shows that throughout nearly the entire 50 week planning horizon, the closure policy cycled between 3, 4, and 5, while spending the most time in 5 (i.e., shelter in place). Furthermore, social distancing and wearing masks were enforced 70% of the time. When it comes to travel policies, the model almost always selected stricter policies. The no travel policy, 4, was selected 78% of the time with Atlantic travel, 3, being selected 20% of the time. The third row in Figure 4.3, shows the progress of cumulative infections and spending over time for the high budget scenario. The cost over the planning horizon is linear while the infections have a few spikes but remain low over all. Starting at budget 8 ($7,472,518,655), the model spent 91.11% of the budget, however, as the budget increased, less of the overall budget was used with scenario 11 spending only 74.5% of the total budget.

When the budget is cut to the medium range ($2 billion to $6 billion), the closure policies become more dynamic and proactive. Instead of the strict closures, the model recommended alternating between strict and lenient closure policies. In particular, a no closure policy is implemented for a few weeks, followed by a partial closure for another week or two. This pattern clearly demonstrates an attempt to contain outbreaks as they reach a critical level, then relaxing the closure policy to salvage the economy, a strategy that might be suitable to countries with modest financial resources. Interestingly, the "shelter in place" closure policy was selected only 4% of the time, likely due to its high cost. It is also interesting to note that even when the budget is significantly reduced, the stricter protection policy (practice social distancing and wear masks) remained unchanged, being implemented 74% of the time. This policy has one of the lower financial impacts as it does not force businesses to close, but modify their operations and capacity to ensure patrons are able to social distance. It also has a high impact on spread because it reduces the transmissibility from 15.6%

to 5.4%. Therefore, having people social distance and wear masks should always be enforced. Finally, travel policies oscillated between all four levels with some negative correlation between the travel and closure policies, meaning that international and domestic travel is more likely to be allowed during closure weeks and prevented when there is no closure. Row 2 in Figure 4.3 shows the progress of infections and spending over time for the chosen medium budget scenario ($1,868,129,664). One can see that the proactive interventions recommended kept the growth in cumulative infections almost linear, as opposed to the exponential growth expected without them. The cumulative infections remained below 3000, and the cost is seen to be cyclical to match the increases and decreases in policy strictness.

Finally, the low budget scenario oscillated between closure policies 1 (27/50 weeks) and 2 (23/50 weeks). This is expected since closures are extremely expensive. Like the two other scenarios, social distancing and wearing masks were recommended but only in a cyclical pattern during the first 16 weeks of the planning horizon. This is likely from the model trying to reduce infections as long as possible but not having sufficient budget to implement the protection policy for longer. The travel policies recommended are generally more relaxed than in the other scenarios, ranging between international travel and national travel. Row 1 of Figure 4.3 shows the progress of infections and spending over time for the low budget scenario. Spending sprees were observed whenever a strict closure policy was implemented. The cumulative infections increased more than 200 times compared to the medium budget case. The strategic interventions implemented were sufficient to reduce infections, however, exponential growth was still observed.

The results obtained can, to a great extent, explain the pandemic pattern observed in NS, where a high value was placed on minimizing infections and ensuring that cases did not exceed healthcare capacity. The economic impact was considered secondary to the healthcare impact. This is evidenced by the strict long term policy strategy put in place while there were few identified cases and maintained until the total active cases began to drop. Between March 4, 2020 and Mach 22, 2020 the Government of NS implemented various restrictions limiting interactions until finally declaring a provincial state of emergency. At this point, there was a maximum limit of five people gathering, several businesses were closed or limited to contactless service, and

movement outside the home was greatly restricted. These measures remained in place until May 2020 when restrictions began to relax. The responsiveness and strict policy strategy was able to drive the total active cases from a peak of 422 on April 24, 2020 to zero by June 22, 2020 (5).

4.2 SA to Optimize State-Based Response Strategies

The time-based framework in section 4.1 has advantages and disadvantages that impact its applicability to real life situations. The entire strategy is determined at the beginning of the planning horizon, which can be beneficial as it allows people to prepare for moving between restrictions. However, this means that the strategy is inflexible and does not account for uncertainty. There are scenarios that the SEIR compartmental model does not account for, such as super spreader events, which could have a major impact on policy restrictions. An alternative approach to the time-based framework is a state-based framework which chooses policy restrictions based on the current state of the system. The current state could be defined as the number of new infections, the number of deaths, number of new hospitalizations, or another metric. The number of new infections was chosen over other metrics due to the fact that the infections are identified before a case reaches hospitalization or death and allows for faster reaction to surges in cases. An example of a state-based strategy is what NS has implemented throughout the COVID-19 pandemic by modifying restrictions based on increases or decreases in infections.

The state-based simulation-optimization framework was created using a similar SEIR compartmental model, however, policy levels were used instead of having individual closure, protection, and travel policies. There are 6 policy levels, each with a specific combination of all three policy types at varying strictness's. The levels were derived by reviewing the policy combinations implemented within NS and are provided in Table 4.7. The framework determines optimal thresholds for changing between the policy levels based on the cumulative cases in the previous time period, which was set at 1 week. Thresholds were chosen for shifting between policies instead of having policies be a direct function of new infections, meaning the model is not constantly oscillating between policies and does need to move in steps. The state-based framework has 10 limit variables that need to be optimized:

1. Limit moving from level 1→2 (UL12);
2. Limit moving from level 2→1 (LL21);
3. Limit moving from level 2→3 (UL23);
4. Limit moving from level 3→2 (LL32);
5. Limit moving from level 3→4 (UL34);
6. Limit moving from level 4→3 (LL43);
7. Limit moving from level 4→5 (UL45);
8. Limit moving from level 5→4 (LL54);
9. Limit moving from level 5→6 (UL56);
10. Limit moving from level 6→5 (LL65);

The limits are separated by policy because it allows for gradual implementation of restrictions that are tailored to the current state of infections. For example, if a surge of 20 cases occurs, the next policy level can be implemented and the resulting cases that week will show if the increased restrictions was sufficient to stop the spread. If the cases continue to rise and there are 30 new cases, then restrictions can be tightened further until the outbreak is stifled, where restrictions will begin to relax. The limits were also separated into upper limits and lower limits because restrictions should be increased when there are rises in cases, and restrictions should be decreased when there is a reduction in cases.

Table 4.7: Summary of policy levels implemented in NS

	Level 1	Level 2	Level 3	Level 4	Level 5	Level 6
Closure	1	1	2	3	4	5
Protection	1	2	2	2	2	2
Travel	1	2	3	3	4	4

A few different optimization algorithms were considered including: GA, Tabu Search (TS), and SA. The GA method is a population-based method that generates and evaluates solutions randomly, which inevitably leads to many solutions that do

not make sense, such as the lower limits being larger than the upper limits. The randomness and the reduction in variables to 10 limits meant that GA was not the most effective optimization approach. Whereas with the neighborhood-based methods of TS and SA, if the current solution is sensible, most of its neighboring solutions will also be sensible. SA was selected over TS because it selects neighbor solutions at random to search the neighborhood, whereas TS requires the entire neighborhood to be enumerated (22). As well, the SA moves in small (and largely controllable) steps, whereas GA makes erratic moves all over the search area.

The SA algorithm functions by starting with an initial solution of upper and lower limits. The neighbor solutions are defined by a change of plus or minus 1 on each limit value, meaning if UL12 starts at 30 the immediate neighbors are 31 and 29. In each iteration 10 random numbers are generated that determine if a limit will move to either neighbor or remain at its current value. The probability that a limit moves to either neighbor is 0.1 each, and the probability the limit remains the same is 0.8. The purpose of having low probabilities for moving to neighbors is that it allows for the neighborhood to be searched gradually. After a new solution is generated, the solution fitness, defined as cumulative infections, is calculated. The algorithm then compares the fitness of the new solution to the fitness of the current solution. If the new solution is more fit, then the current solution shifts to the new one. If the new solution is less fit, then the current solution moves to the new solution with the probability pa or remains the same with probability $1 - pa$. Incorporating the probability pa allows non-improving solutions to be accepted in the hope of it leading a better solution. The function for pa is provided in equation 4.11 where Z_c is the fitness of the current solution, Z_n is the fitness of the new solution, and T is the temperature.

$$pa = \exp \frac{Z_c - Z_n}{T} \tag{4.11}$$

The probability pa changes over time with temperature T. It starts high to frequently allow non-improving solutions but decreases over time which puts more emphasis on moving to more fit solutions. The temperature T_0 must be initialized at a sufficiently large value, a rule of thumb is it should be large in comparison to typical values of $\mid Z_c - Z_n \mid$ (22). The temperature then decreases over each iteration according to a temperature schedule. The algorithm concludes when the entire temperature

Table 4.8: A pseudocode of the simulated annealing process

Inputs

Initial solution C
Initial temperature T_0
Temperature schedule $f(T)$
Number iterations i at each T
Iteration stopping rule s

Code

```
1   While counter < s do
2     Generate a neighbor solution N
3     if N fitness ≥ C fitness then
4       C = N
5     else
6       C = N with pa= e^((Cfitness−Nfitness)/T
7     end if
8     counter=counter+1
9     if remainder(counter/i) = 0 then
10      T=f(T)
11    end if
```

schedule has been run through. A pseudocode for the SA algorithm can be found in Table 4.8.

The starting solution was created by reviewing the results of the time-based optimization. Three budgets were chosen, \$1.3B, \$3.2B, and \$7.5B. The strategy and weekly infections for each budget were analysed to determine at what number of cases in the previous week was there a shift upward or shift downward in policy strictness. Reconciling when policies shifted in the time-based framework to the state-based framework was challenging because the time-based framework uses disaggregate policies whereas the state-based framework uses aggregate policy levels. An assumption was made that using the closure policy shifts would be close to the level shifts because the main difference is that policy levels 1 and 2 use closure policy 1 as seen in Table 4.7. Therefore, it was assumed policy levels 1 and 2 would have the same upper and lower limits. Another challenge was that there was missing data for some limits as not every strategy shifted between all 10 limits. For example, with a budget of 1.3\$B only shifts between closure policies 1 and 2 were observed. Table 4.9 shows the limits derived from the time-based optimization. Budget 4 was the only one which provided a semi viable initial solution, however, not all the limits made sense. For instance, UL34 was 53 and UL45 was 32, meaning even if the weekly cases decrease by 21 there will still be a shift upward to a stricter policy level. This solution was used as a basis

for a more logical initial solution which is provided in the last row of table 4.9.

Table 4.9: Initial limit solutions derived from the time-based optimization results for the low, medium, and high budgets

	UL12	UL23	UL34	UL45	UL56	LL65	LL54	LL43	LL32	LL21
Budget 2.1	23494.25	23494.25	NA	NA	NA	NA	NA	NA	14652.49	14652.49
Budget 4	29.13	29.13	53.39	31.99	NA	11.57	18.05	34.52	20.26	20.26
Budget 8	0.34	0.34	0.00007	0.17	0.33	0.26	0.001	0.17	0.17	NA
Generated	20	25	30	35	40	10	15	20	15	10

A budget constraint is implemented in the SA using a penalty function that penalizes infeasible solutions by reducing their fitness values, in this case number of cumulative infections from a strategy, in proportion to the violation of the constraint. Only dynamic penalties were considered as this algorithm functions similarly to the GA by searching for improving solutions and an initial move might be over budget, but could lead to a better solution within budget. The dynamic penalty will start small to allow over budget strategies, but will increase over time to slowly weed out infeasible solutions. The same penalty value of 0.00001 was used from the time-based framework, and a small analysis was completed testing different dynamic penalty functions. The functions and their results are found in Table 4.10. The second dynamic penalty function was selected as it resulted in the fewest cumulative infections.

Table 4.10: SA dynamic penalty functions and cumulative infections

Penalty Function	Minimum Cumulative Infections
$0.00001 \times \text{counter}$	889
$0.00001 \times \frac{counter}{2}$	821
$0.00001 \times counter^2$	841

The initial temperature should be large compared to $\mid Z_c - Z_n \mid$ as this will encourage an almost random search through the feasible region (22). Therefore, an initial temperature of 3×10^9 was selected. The number of iterations at each T value was defined as 10 as it is common to select 5 or 10. The temperature schedule was optimized using parameter tuning and testing different rates at which T decreases. To ensure the *pa* was small near the end of the run, the temperature schedule always decreased until reaching $T < 1$. This ensures non-improving solutions will not be selected near the end of the optimization run, and puts emphasis on only moving to better solutions. There were three temperature schedules tested and 5 trials of each schedule were run. The schedules and results of the parameter tuning are provided

in Table 4.11. Temperature schedule 2 found the best solution and was used in generating the results.

Table 4.11: SA parameters used in parameter optimization trials and results of each trial

	1	2	3
Initial T	3,000,000,000	3,000,000,000	3,000,000,000
T Function	$T_{new} = 0.3T_{old}$	$T_{new} = 0.75T_{old}$	$T_{new} = 0.5T_{old}$
Number of T values	20	80	35
Iterations at each T	10	10	10
Total Iterations	200	800	350
Minimum Cumulative Infections	848	821	860

4.2.1 Results

This section presents the results obtained from implementing the state-based framework. The framework was run using four different initial solutions which are provided in table 4.12. Each initial solution was run 5 times and had a budget of $1,000,000,000. Initial solutions 1, 3, and 4 generated optimal strategies. Figure 4.4 shows a snippet of the SA for initial solution 1 around the optimal solution. Detailed results for the state-based approach can be found in Appendix C.

Table 4.12: SA initial solutions of upper and lower limits for shifting between policy levels

	UL12	LL21	UL23	LL32	UL34	LL43	UL45	LL54	UL56	LL65
1	20	10	25	15	30	20	35	15	40	10
2	25	15	30	20	35	25	40	20	45	15
3	15	5	20	10	25	15	30	10	35	5
4	30	10	35	15	40	20	45	15	50	10

4.2.2 Analysis

The results seen in Figure 4.4 show that there are multiple combinations of lower and upper limits that will produce the minimum cumulative infections. This is because the combinations generate the same policy level strategy which is provided in Figure 4.5. The policy levels immediately move up in the first 3 weeks then maintain level 4 restrictions for 4 weeks. It then decreases to level 2 where it maintains a steady state where cases that are too high to move down to level 1, but too low to move up to level

UL12	LL21	UL23	LL32	UL34	LL43	UL45	LL54	UL56	LL65	Cost	Infections	Penalized Infections
24	7	47	22	37	14	30	10	40	5	732523090	928	928
24	7	47	22	37	14	30	10	40	4	732523090	928	928
25	7	47	22	37	13	30	11	40	4	732523090	928	928
25	7	47	22	37	13	31	11	39	4	732523090	928	928
25	7	47	23	37	12	31	11	39	4	847879507	860	860
25	7	46	24	37	11	31	12	39	4	847879507	860	860
25	7	45	24	37	12	31	12	39	4	847879507	860	860
25	7	44	25	37	12	31	12	39	4	847879507	860	860
26	7	44	24	38	12	31	12	38	4	847879507	860	860
26	8	44	24	38	12	31	12	38	4	847879507	860	860
26	8	43	24	38	12	31	12	39	4	847879507	860	860
26	7	43	24	38	12	31	12	39	5	847879507	860	860
26	7	43	24	38	12	31	12	39	5	847879507	860	860
26	7	43	24	37	12	31	13	40	5	847879507	860	860
26	7	43	23	36	12	31	13	40	5	847879507	860	860
26	7	43	23	36	12	31	13	40	5	847879507	860	860
26	7	44	24	35	12	31	13	40	6	847879507	860	860
26	7	45	24	35	12	31	12	40	6	847879507	860	860
26	7	44	24	35	12	31	12	40	6	847879507	860	860
26	7	44	25	35	12	31	12	40	6	847879507	860	860
26	7	44	25	35	12	30	11	40	6	847879507	860	860
26	6	44	25	35	12	30	11	40	6	847879507	860	860
26	6	44	25	35	11	31	11	40	7	847879507	860	860
26	6	44	24	35	11	30	11	39	8	847879507	860	860
26	7	44	24	35	11	30	11	39	7	847879507	860	860
26	7	44	24	35	11	30	11	38	7	847879507	860	860
26	7	44	25	35	10	30	11	38	7	847879507	860	860
25	7	44	25	35	9	30	11	39	7	847879507	860	860
26	6	44	25	34	9	30	11	39	7	847879507	860	860
26	6	44	25	34	9	30	11	39	7	847879507	860	860
26	6	44	25	34	9	30	12	39	7	847879507	860	860
26	6	45	25	34	9	30	12	39	7	847879507	860	860
26	6	46	25	34	9	30	12	39	7	847879507	860	860
26	6	46	26	34	9	30	12	39	7	847879507	860	860
26	6	46	26	34	8	30	11	39	7	847879507	860	860
26	6	46	25	34	8	30	12	39	7	847879507	860	860
26	6	46	26	35	8	31	12	39	7	847879507	860	860
26	6	46	25	36	8	31	12	40	7	847879507	860	860
26	6	46	25	36	8	31	12	40	8	847879507	860	860
25	6	45	26	37	7	31	12	39	8	847879507	860	860
25	6	45	26	37	7	31	13	38	9	847879507	860	860
24	5	45	26	36	7	31	13	38	9	847879507	860	860
24	5	45	26	36	8	31	13	38	9	847879507	860	860
24	5	45	25	37	8	31	13	38	9	847879507	860	860
24	5	45	25	37	8	31	12	37	9	847879507	860	860
24	5	45	25	37	7	31	12	36	8	847879507	860	860
25	5	45	25	37	6	31	12	35	9	963235924	821	821
24	5	45	25	37	6	31	12	35	9	963235924	821	821
24	5	45	25	37	6	31	12	35	8	963235924	821	821
24	5	45	25	37	7	31	12	35	8	847879507	860	860
24	5	45	25	37	7	31	12	36	8	847879507	860	860
24	5	45	25	37	7	32	12	36	8	847879507	860	860

Figure 4.4: Subsection of SA output for initial solution 1

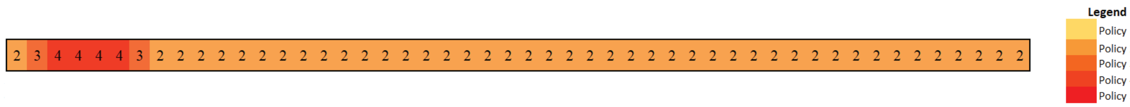

Figure 4.5: Weekly policy level strategy heatmap over a 50 week horizon

3. This can be explained from the initial number of cases being significant enough to cause wide spread, so the model immediately moves to strict restrictions where the active cases will decrease. By week 7 there are few enough infected individuals to relax restrictions so the policy level decreases until it reaches level 2.

Though there are several combinations of limits, there are trends that can be observed among them. The lower limits generally do not get very high, meaning the cases need to drop significantly to trigger a relaxation in restrictions. For example the range on LL21 is [0,10] and LL43 is [4,6]. The outlier is LL32 which has a range of [5,35], however, this could be attributed to the fact that restrictions are not relaxed enough to cause a spike in cases when moving from level 3 to level 2, so the number of cases does not need to be as low. Also the UL12 is the lowest with a range of [1,26] meaning the model wants to quickly move into level 2 given a few cases in a week. Another observation is that UL23 is typically the largest with a range of [20,53] meaning there needs to be a jump in cases from the previous week to trigger a shift into policy level 3.

The limits generated through the SA are similar to what has been observed in NS. Restrictions have often been increased quickly after small spikes in weekly cases. In particular, during the second wave in November 2020, restrictions were increased after 26 cases in a week (21). They were further increased after 111 cases in the following week and maintained for 3 to 4 weeks until slowly relaxing. NS has also never reached a point where restrictions have been completely removed, social distancing and wearing masks, as well as travel restrictions continue to be enforced.

Chapter 5

Scenario Testing

Mathematical models are being developed to predict the spread of COVID-19 and determine its potential economic impact and impact to health care systems. Specifically, SIR and SEIR models are commonly being used to predict the spread of the COVID-19 and the impact on health care resources (28; 10; 33; 55). Modelling is also being used to determine the impact of policy decisions on the spread of the virus (56; 14; 58). An extension was added to the modified, age-stratified SEIR simulation model described in Chapter 3 which encompasses the proposed vaccine rollout schedule within NS. The updated conceptual model is provided in Figure 5.1. The extended model allowed for testing several different policy scenarios and their impact on infections, hospital resources, and cumulative deaths. The difference between this part and the remainder of the thesis, apart from including the vaccine rollout, is that it does not try to optimize the response strategy, but merely compare a few pre-determined opening strategies. This should become clear at the outset. It could, however, be incorporated in an optimization framework like the previous cases, which is something that was not done but can become a potential future extension.

5.1 Methodology

The extended compartmental model considers the efficacy of the vaccine, the proportion of the NS population that will voluntarily receive a vaccine, and the age groups eligible to receive a vaccine. The vaccination stream pulls from the susceptible group and moves individuals directly into the recovered group. The vaccination schedule was built into the model using NS's existing and planned vaccination rollout. The initial phases focused on frontline workers who had an increased likelihood of encountering infected individuals and residents of long-term care (LTC) facilities. Frontline or high risk workers can include but are not limited to nurses, physicians, firefighters,

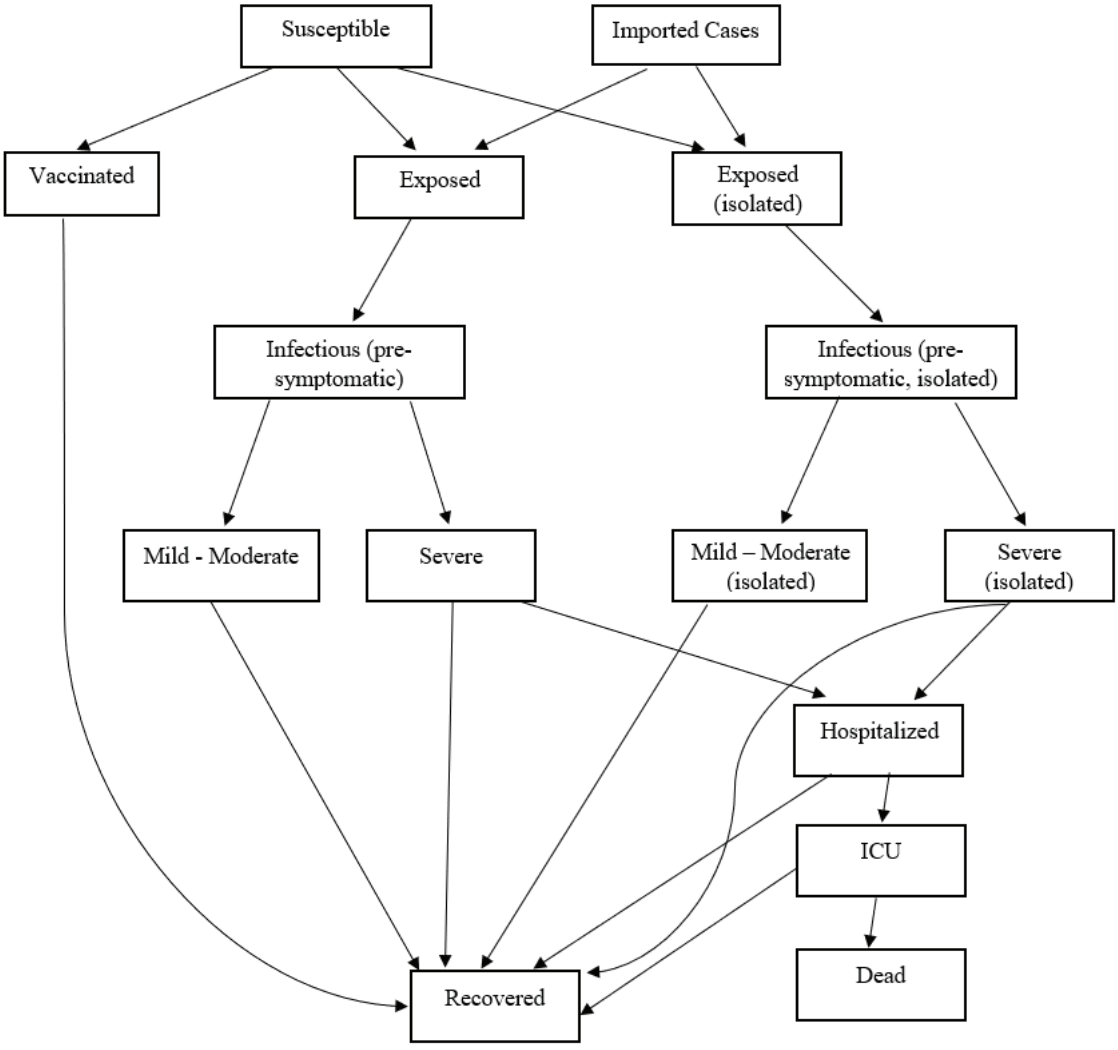

Figure 5.1: Conceptual SEIR model of COVID-19 with vaccination

and police officers. It is estimated through consultation with NSHA that the vaccinations completed in the initial phases targeted people over 80 in LTC facilities and workers aged 20-59. The last phase of the rollout is age-based only, starting with people over 80 and proceeding downward in 5-year increments. The entire eligible population was expected to have access to their first vaccine by June 30, 2021 (19). There were three vaccines approved for use by Health Canada that were distributed in NS (18). The first, Pfizer-BioNTech, was approved for individuals 16 and up as of December 9, 2020 then expanded to individuals 12 and up on May 5, 2021. The second vaccine, Moderna, was approved for individuals 18 and up as of December 23, 2020. The final vaccine, AstraZeneca, was approved for individuals 18 and up on February 26, 2021, however, was discontinued in NS on May 12, 2021. The initial eligible population was individuals over 15, however, due to the changes with Pfizer-BioNTech it was updated to individuals over 11 and is reflected in the model. The minimum daily vaccinations by age group needed to meet the June deadline was determined and the resulting vaccination schedule was modeled. The second vaccine dose (or completed vaccine) will occur a maximum of 4 months later, which models the worst-case scenario. This model has given a general vaccine efficacy of 85% at the first dose, and efficacy of 92% at the second dose which is an approximation of the vaccines that were being used in NS (Pfizer-BioNTech, Moderna, AstraZeneca). The efficacy is modeled by only moving a portion of those vaccinated into the recovered compartment, meaning on 85% of the individuals that get a their first dose will be immune. Initially, it was assumed that 80% of the population would choose to get a vaccine, however, this was updated to 90% of the population to better reflect the reality in NS. The minimum target set by the Chief Medical Officer of NS, Dr. Strang, is 75% of the overall population which equates to approximately 85% of the eligible population (20).

The scenarios were derived in consultation with NSHA to provide insight on the health implications of relaxing restrictions at different periods during the vaccination rollout. The health implications included cumulative infections, active infections, hospital admissions, and deaths. The simulation was run using the Vensim model (Figure 5.2). The scenarios were run starting from March 15, 2021.

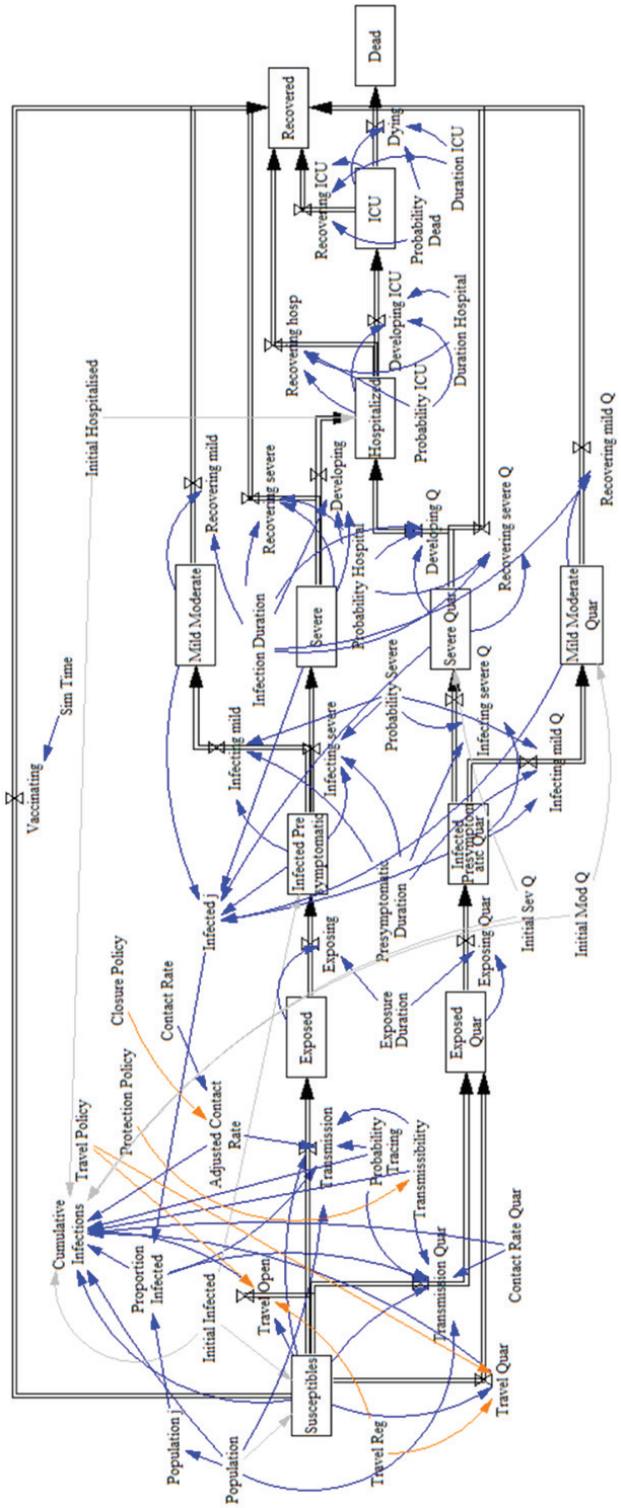

Figure 5.2: Vensim compartmental model of COVID-19 with vaccination

5.2 Results

Figure 5.3 shows the results of four conservative approaches to the relaxation of restrictions. The top row of Figure 5.3, shows the results if there were no changes to the current restrictions, as of March 15, 2021, in terms of closure level, continued use of masks and social distancing, and a 2-week quarantine for travellers from outside of the province. This yields only a small number of active cases, 22, that is at its peak at the beginning. The second row of Figure 5.3 shows the results with loosening of travel restrictions by allowing travel from Atlantic Canada without quarantine restrictions (Atlantic Bubble) on April 15, 2021. This yields essentially identical results to the first scenario. The third row of Figure 5.3 goes further by loosening both closure and opening the Atlantic Bubble on April 15, 2021, which yields only an additional 11 cases from the first two scenarios. The final row of Figure 5.3 shows the results from maintaining restrictions until May 14, 2021, opening the Atlantic Bubble until June 30, 2021, and opening national travel until July 5, 2021 where international travel is opened. The closure policy is loosened on June 30, 2021 and the protection policies are kept in place. This yields a maximum of 22 active infections which peaks on March 15, 2021 and 86 cumulative infections. None of these scenarios resulted in any hospitalizations.

Figure 5.4 shows the effects of less restrictive policy options. The top row of Figure 5.4 shows the effects of opening the Atlantic Bubble on May 14, 2021, opening to national travel on July 1, 2021, and moving to the least strict closure level on September 1, 2021. This results in a steady increase in cases from July 9, 2021 with 572 cumulative infections after one year. A small number of hospitalizations result from this scenario with 2 deaths over the year. The second row of Figure 5.4 shows the effects of opening the Atlantic Bubble on May 14, 2021, opening to national travel on July 5, 2021 and moving to the least strict closure level on September 3, 2021. It then toggles between removing and invoking the mask and social distancing policy starting October 18, 2021 to January 16, 2022 where it removes masks and social distancing. This results in a delayed active infection peak of 6,010 on June 11, 2022 and 103 hospitalizations on July 2, 2022. The third row of Figure 5.4 shows the effects of opening the Atlantic Bubble and loosening the closure policy on May 14, 2021, opening to national travel on July 5, 2021, and removing the mask and social

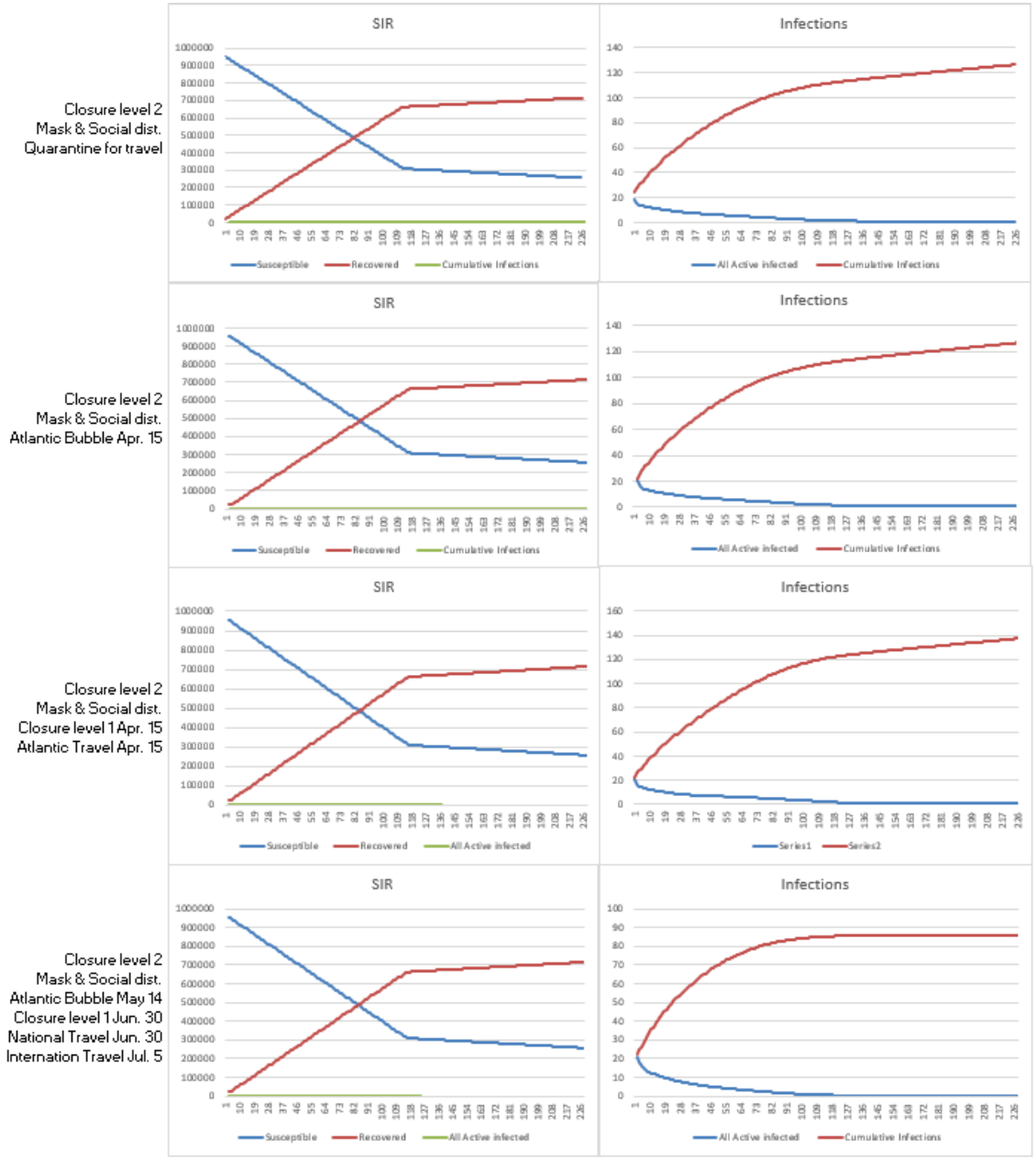

Figure 5.3: Model outputs with conservative policy scenarios from March 15 2021; the charts on the left show the change in the number of people susceptible, infected, and recovered; the charts on the right show the active and cumulative infections over time in NS.

distancing policy on September 13, 2021. This results in peak active infections of 6,115 by February 16, 2022 and 105 hospitalizations on March 8, 2022. The fourth row of Figure 5.4 shows the results from immediately opening the Atlantic Bubble, opening all businesses without restrictions, and the removal of the mask and social distancing policy. This yields a maximum of 72,913 active infections on May 29, 2021 and a maximum of 1109 hospitalizations on June 13, 2021.

5.3 Analysis

These results indicate that closure levels, protection through masks and social distancing, and restricting travel, all impact the number of COVID-19 infections and hospitalizations. The first two rows in Figure 5.3 demonstrate that quarantine does not have a significant impact on infections if other restrictions are kept in place. By maintaining an Atlantic Bubble along with masks and social distancing, the model predicts NS will have a negligible rise in infections, even when restrictions on businesses and gatherings are loosened during the vaccination period. From a policy perspective, this means that the mandatory quarantining for travellers can be removed safely if the closure and protection restrictions are followed. The results of the third conservative scenario suggest that as long as the mask and social distancing policy is maintained while closure and travel restrictions are loosened, NS will only see a small steady rise in the cumulative infections without any significant hospitalizations. However, if the mask and social distancing policy are removed by the fall, the remaining unvaccinated population will drive a large surge in infections. This will result in approximately 6,010 peak active infections, cumulative infections of 70,341, and a peak of 103 hospitalizations by March 2022. This is lower than the impact of removing restrictions immediately, which would result in 72,913 peak active infections, 328,405 cumulative infections, and 1,109 hospitalizations. These results show that if restrictions are opened too soon, a surge in cases will occur before herd immunity can be met through vaccination. The liberal policy results indicate that masks and social distancing will be required in order to continue to keep the case count and hospitalizations low, as closure and travel policies are relaxed. The policy implications from the strategy testing can still provide insight for policy decisions on new mutations of COVID-19 such as the delta variant. The delta variant is more infective than the

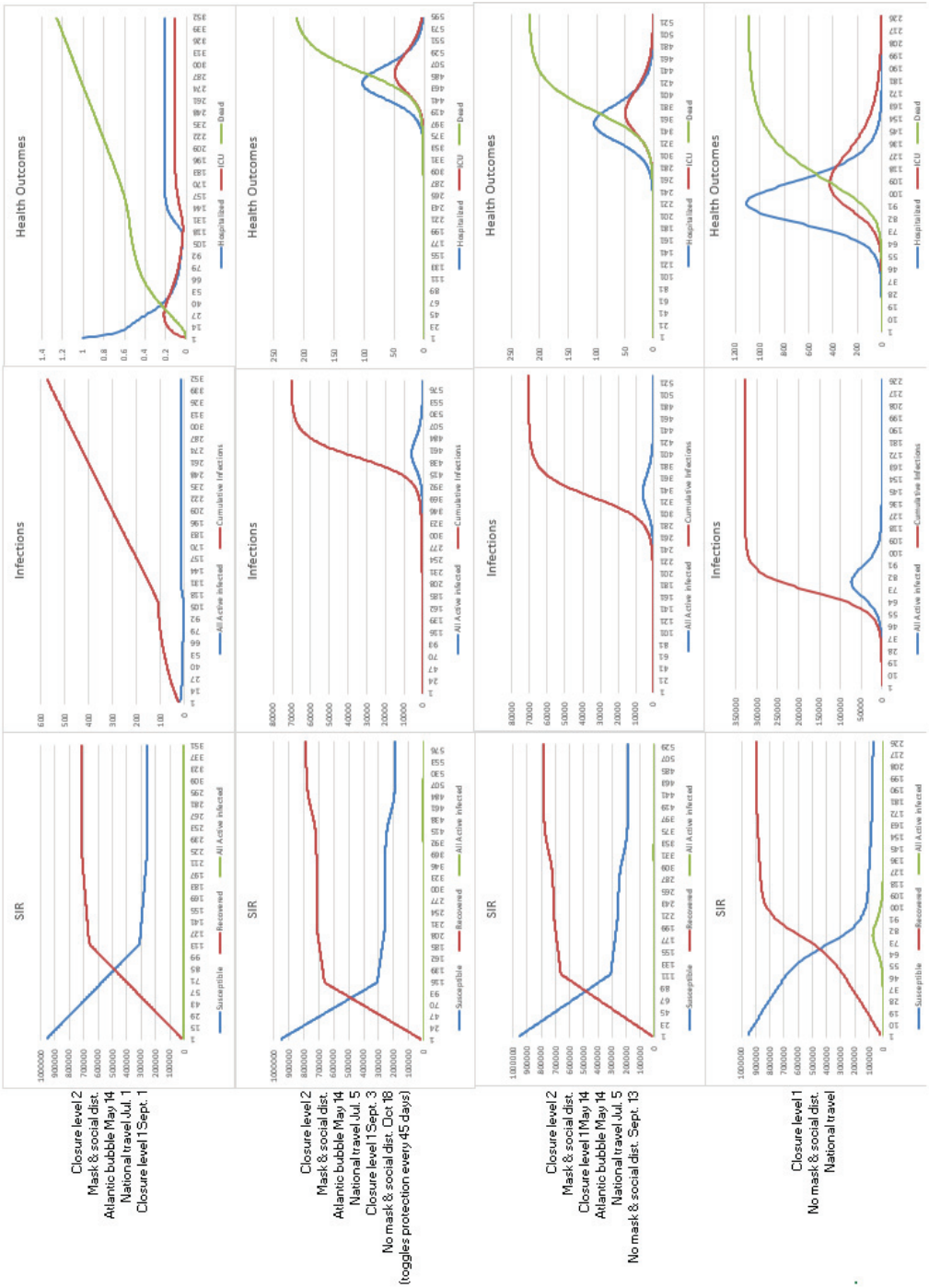

Figure 5.4: Model outputs with liberal policy scenarios from March 15 2021; the charts on the left show the change in the number of people susceptible, infected, and recovered; the charts in the middle show the active and cumulative infections; and the charts on the right show the hospitalizations, ICU admissions, and deaths over time in NS.

original variant meaning the policy decisions should be at least as strict as the ones derived from the strategy testing. Therefore, if the delta variant were to start a fourth wave in NS, it is important to continue to enforce social distancing and masks as seen in the conservative scenario testing. There should also be further incentives for Nova Scotians to get vaccinated, as of August 2021, while older age groups have uptake as high as 99% the younger populations have as few as 53% (20).

Chapter 6

Conclusions and Extensions

This chapter draws some insights and conclusions based on the results obtained from the simulation-optimization and the scenario testing experiments. It also proposes some future extensions for both research themes.

6.1 Simulation-Optimization

In this thesis, a simulation-optimization framework for optimizing response strategies to epidemics is presented and applied to devise response strategies in NS to the COVID-19 outbreak. The proposed framework combines a modified, age-stratified SEIR compartmental model to evaluate dynamic response strategies that include different levels of closure, protection, and travel policies with metaheuristic algorithms that iteratively search for better strategies. Response strategies were evaluated based on both their health and economic impact, represented by the total number of infections, and their economic cost. The results for the time-based strategies showed a clear trade-off between health and economic objectives, and the model proposed different strategies depending on the available budget. Under the high budget scenario tested, stricter closure policies were recommended throughout nearly the entire planning horizon, whereas under low and medium budget scenarios, it swung between no closure and partial closures, trying to suppress disease outbreaks while giving the economy some room to breathe. The medium budget results show that even if a region does not have a large budget, through cyclical implementation of restrictions cases can be kept within a manageable range 2,600 cumulative infections to 250 cumulative infections over a 50 week period. Social distancing and wearing masks were almost always recommended with medium and high budgets. Therefore, wearing masks and social distancing should always be enforced for regions with a sufficient budget. The travel policy was always enforced in an oscillating pattern, but was less sensitive to the budget when strict closure policies were in place. This means if policymakers

are enforcing strict travel regulations closures could be relaxed a or vice versa. The Atlantic Bubble is a real implementation of this approach where travel was relaxed while closures were maintained at more strict levels. Along with prescribing (near-)optimal strategies under budget constraints, this tool can also help policymakers leverage existing capacity and plan for peak cases.

As the time-based framework is limited by the fact the entire strategy is determined at the outset, a state-based framework was also developed. This framework finds (near-)optimal policy level thresholds for shifting between restriction levels. It was also applied to the COVID-19 outbreak in NS. Threshold limits were evaluated in terms of their health impact and economic cost. The results show that the lower limits should be small, generally in the range of [0,20]. This ensures the outbreak has been reduced enough that relaxing restrictions will not lead to a large influx in cases. The best way to allocate funds is to have limits that immediately stifle an outbreak with strict restrictions, then move to a low level as soon as possible where active cases will reach a steady state. The initial upper limit should also be small so to quickly increase restrictions to prevent the spread from becoming exponential. The threshold limits can be used in conjunction with the time-based strategy by prescribing an optimal policy strategy, then updating restrictions according to thresholds if there is significant deviation from the initial strategy. The simulation model used does not consider unique scenarios such as super spreader events, therefore, if one were to occur the strategy could be updated according to the thresholds.

The proposed GA and SA frameworks are quite generic and can be easily tailored for other epidemics or jurisdictions. The current population demographics such as the number of people in each age category and proportion of people with at least one comorbidity by age can be changed to evaluate the response strategies in a different region. To model a different disease, the disease parameters such as the latent period, infection period, and probability of death can be modified to evaluate another virus. This could be expanded to include the delta variant of COVID-19 by increasing the transmissibility, or having a stream from recovered back to susceptible if previously infected individuals are still susceptible to becoming infected. Furthermore, other epidemiological models might be utilized, along with alternative optimization techniques. The epidemiological model could be modified to include seasonality by increasing or

decreasing the likelihood of transmission given the season, or include a spatial component. The spatial aspect could be included by having multiple populations that are interconnected such as major cities within a province. The SA optimization could be extended to a multi-start SA algorithm which has multiple initial solutions that are run simultaneously and prevents getting stranded in a poor area of the search space. Another potential, and quite interesting, extension of the compartmental model is to include vaccination, which has recently become a viable alternative at the disposal of policymakers for the COVID-19 pandemic. This can be done by adding a direct flow from the Susceptible to the Recovered compartments that is regulated through a vaccination policy to be selected. The state-based framework could also be updated to allow for the policy level to move to any level instead of the immediate neighbor levels. Finally, a more accurate calibration of the economic burden of policies can be performed to capture issues like the interactions between different classes of policies and the nonlinear cost as a function of the implementation duration of a given policy.

6.2 Scenario Testing

The modified, age-stratified SEIR compartmental can be used by decision makers to test and compare different policy strategies within NS. The health implications of each scenario is estimated, which can help with selecting a policy strategy and resource planning. The scenarios tested range from gradual relaxation of restrictions to immediate removal. The results of the first two conservative model scenarios show that requiring quarantine for travellers has negligible impact on cumulative infections if other restrictions remain in place. This means the quarantine period for travellers can be removed if masks and social distancing are enforced and closures are not fully relaxed. The closure and travel restrictions should be relaxed gradually through the vaccination rollout or there will be a large surge in cases, as predicted in liberal policy scenario 4. After a sufficient number of people are vaccinated, loosening restrictions results in minimal infections among the remaining population as long as social distancing and masks are enforced. If social distancing and masks are removed, as seen in liberal strategies 2 and 3, there is still a smaller wave with a peak active cases of around 6000 that is predicted. Therefore, policymakers should incentivize vaccinations in age groups where the uptake is low to minimize the size of a potential

fourth wave.

The model uses a basic vaccination rollout plan based on the initial immunization plan outlined by the Government of NS. The initial plan is conservative and could be improved by using actual data to reflect the rate at which people were and are being vaccinated.

Bibliography

[1] Adiga, A., Dubhashi, D., Lewis, B., Marathe, M., Venkatramanan, S., and Vullikanti, A. Mathematical models for COVID-19 pandemic: A comparative analysis. *Journal of the Indian Institute of Science 100*, 4 (Oct, 2020), 793—807. doi:10.1007/s41745-020-00200-6.

[2] Bertsimas, D., Ivanhoe, J., Jacquillat, A., Li, M., Previero, A., Lami, O. S., and Bouardi, H. T. Optimizing vaccine allocation to combat the COVID-19 pandemic. *medRxiv* (Nov, 2020). doi:10.1101/2020.11.17.20233213.

[3] Bhatia, R., and Klausner, J. Estimating individual risks of COVID-19-associated hospitalization and death using publicly available data. *PLOS ONE 15*, 12 (Dec, 2020), 1–12. doi:10.1371/journal.pone.0243026.

[4] Brauer, F., and Castillo-Chavez, C., Eds. *Mathematical Models in Population Biology and Epidemiology*. Texts in Applied Mathematics. Springer, 2012.

[5] Campbell, M. NS COVID-19 Timeline. *Cape Breton Spectator* (Mar, 2020). http://capebretonspectator.com/2020/03/25/covid-19-timeline/.

[6] Chu, D. K., Akl, E. A., Duda, S., Solo, K., Yaacoub, S., Schünemann, H. J., El-harakeh, A., Bognanni, A., Lotfi, T., Loeb, M., Hajizadeh, A., Bak, A., Izcovich, A., Cuello-Garcia, C. A., Chen, C., Harris, D. J., Borowiack, E., Chamseddine, F., Schünemann, F., Morgano, G. P., Muti Schünemann, G. E. U., Chen, G., Zhao, H., Neumann, I., Chan, J., Khabsa, J., Hneiny, L., Harrison, L., Smith, M., Rizk, N., Giorgi Rossi, P., AbiHanna, P., El-khoury, R., Stalteri, R., Baldeh, T., Piggott, T., Zhang, Y., Saad, Z., Khamis, A., and Reinap, M. Physical distancing, face masks, and eye protection to prevent person-to-person transmission of SARS-CoV-2 and COVID-19: a systematic review and meta-analysis. *The Lancet 395*, 10242 (2020), 1973–1987. doi:10.1016/S0140-6736(20)31142-9.

[7] Cohen, T., Colijn, C., Finklea, B., and Murray, M. Exogenous re-infection and the dynamics of tuberculosis epidemics: local effects in a network model of transmission. *Journal of The Royal Society Interface 4*, 14 (2007), 523–531. doi:10.1098/rsif.2006.0193.

[8] Dalgiç, O., Özaltin, O. Y., Ciccotelli, W. A., and Erenay, F. S. Deriving effective vaccine allocation strategies for pandemic influenza: Comparison of an agent-based simulation and a compartmental model. *PLOS ONE 12*, 2 (Feb, 2017). doi:10.1371/journal.pone.0172261.

[9] Dimitrov, N. B., Goll, S., Hupert, N., Pourbohloul, B., and Meyers, L. A. Optimizing tactics for use of the U.S. antiviral strategic national stockpile for pandemic influenza. *PLOS ONE 6*, 1 (Jan, 2011), 1–10. doi:10.1371/journal.pone.0016094.

[10] Ediriweera, D. S., de Silva, N. R., Malavige, G. N., and de Silva, H. J. An epidemiological model to aid decision-making for COVID-19 control in Sri Lanka. *PLOS ONE 15*, 8 (Aug, 2020), 1–10. doi:10.1371/journal.pone.0238340.

[11] Ehrgott, M. Scalarization techniques. In *Multicriteria Optimization*. Springer Berlin Heidelberg, 2005, pp. 97–126. isbn:978-3-540-27659-3.

[12] Emmerich, M. T. M., and Deutz, A. H. A tutorial on multiobjective optimization: fundamentals and evolutionary methods. *Natural Computing 17*, 3 (Sep, 2018), 585–609. doi:10.1007/s11047-018-9685-y.

[13] Gallo, L. G., Oliveira, A. F. d. M., Abrahão, A. A., Sandoval, L. A. M., Martins, Y. R. A., Almirón, M., dos Santos, F. S. G., Araújo, W. N., de Oliveira, M. R. F., and Peixoto, H. M. Ten epidemiological parameters of COVID-19: Use of rapid literature review to inform predictive models during the pandemic. *Frontiers in Public Health 8* (Dec, 2020), 830. doi:10.3389/fpubh.2020.598547.

[14] Giordano, G., Blanchini, F., Bruno, R., Colaneri, P., Di Filippo, A., Di Matteo, A., and Colaneri, M. Modelling the COVID-19 epidemic and implementation of population-wide interventions in Italy. *Nature Medicine 26*, 6 (Jun, 2020), 855–860. doi:10.2139/ssrn.3547729.

[15] Global Preparedness Monitoring Board. A World in Disorder. Global Preparedness Monitoring Board Annual Report 2020. Tech. rep., World Health Organization, Geneva, 2020. https://apps.who.int/gpmb/assets/annual_report/GPMB_AR_2020_EN.pdf.

[16] Government of Canada. Asthma in Canada. https://health-infobase.canada.ca/datalab/asthma-blog.html. Accessed: 2020-08.

[17] Government of Nova Scotia. Coronavirus (covid-19): alerts, news and data. https://novascotia.ca/coronavirus/alerts-notices/provincial-state-emergency, Feb, 2021. Accessed: 2020-10.

[18] Government of Nova Scotia. Coronavirus (covid-19): vaccine. https://novascotia.ca/coronavirus/vaccine/approved-vaccines, 2021. Accessed: 2021-03.

[19] Government of Nova Scotia. COVID-19 immunization plan. https://https://novascotia.ca/coronavirus/vaccine/immunization-plan, Mar, 2021. Accessed: 2021-03.

[20] Government of Nova Scotia. Covid-19 vaccine update. https://novascotia.ca/news/release/?id=20210723002, Jul, 2021. Accessed: 2021-07.

[21] Government of Nova Scotia. New restrictions to reduce spread of COVID-19. https://novascotia.ca/news/release/?id=20201120003, Nov, 2021. Accessed: 2021-05.

[22] Hillier, F. S., and Lieberman, G. J. *Introduction to operations research*, 10 ed. McGraw-Hill, 2015.

[23] Kahraman, C., and Topcu, Y. I., Eds. *Operations Research Applications in Health Care Management*. International Series in Operations Research and Management Science. Springer, 2018.

[24] Kaplan, E. Containing 2019-nCoV (Wuhan) coronavirus. *Health Care Manag Sci 23* (Sep, 2020). doi:10.1007/s10729-020-09504-6.

[25] Keimer, A., and Pflug, L. Modeling infectious diseases using integro-differential equations: Optimal control strategies for policy decisions and applications in COVID-19. doi:10.13140/RG.2.2.10845.44000, May, Unpublished results.

[26] Kretzschmar, M., and Wallinga, J. *Mathematical Models in Infectious Disease Epidemiology*. Springer New York, New York, NY, 2010. doi:10.1007/978-0-387-93835-6_12.

[27] Kretzschmar, M., and Wallinga, J. *Mathematical Models in Infectious Disease Epidemiology*. Springer New York, New York, NY, 2010, pp. 209–221. doi:10.1007/978-0-387-93835-6_12.

[28] Lavielle, M., Faron, M., Lefèvre, J. H., and Zeitoun, J.-D. Extension of a SIR model for modelling the propagation of COVID-19 in several countries. *medRxiv* (May, 2020). doi:10.1101/2020.05.17.20104885.

[29] Lee, H. L., and Pierskalla, W. P. Mass screening models for contagious diseases with no latent period. *Operations Research 36*, 6 (1988), 917–928. doi:10.1287/opre.36.6.917.

[30] Liu, H. *The Economic Impact of Travel Restrictions on the Canadian Economy due to the COVID-19 Pandemic*. Oct, 2020.

[31] Long, E. F., and Brandeau, M. L. *OR's Next Top Model: Decision Models for Infectious Disease Control*. 2009, ch. Chapter 6, pp. 123–138.

[32] Malone, J. D., Brigantic, R., Muller, G. A., Gadgil, A., Delp, W., McMahon, B. H., Lee, R., Kulesz, J., and Mihelic, F. M. U.s. airport entry screening in response to pandemic influenza: Modeling

and analysis. *Travel Medicine and Infectious Disease 7*, 4 (2009), 181–191. doi:10.1016/j.tmaid.2009.02.006.

[33] Mbuvha, R., and Marwala, T. On data-driven management of the COVID-19 outbreak in South Africa. *medRxiv* (Apr, 2020). doi:10.1101/2020.04.07.20057133.

[34] Mehrotra, S., Rahimian, H., Barah, M., Luo, F., and Schantz, K. A model of supply-chain decisions for resource sharing with an application to ventilator allocation to combat COVID-19. *Naval Research Logistics (NRL) 67*, 5 (May, 2020), 303–320. doi:10.1002/nav.21905.

[35] Mossong, J., Hens, N., Jit, M., Beutels, P., Auranen, K., Mikolajczyk, R., Massari, M., Salmaso, S., Tomba, G. S., Wallinga, J., Heijne, J., Sadkowska-Todys, M., Rosinska, M., and Edmunds, W. J. Social contacts and mixing patterns relevant to the spread of infectious diseases. *PLOS Medicine 5*, 3 (Mar, 2008), 1–1. doi:10.1371/journal.pmed.0050074.

[36] Nova Scotia Health Authority. *Contact Tracing: Preventing Spread*. Feb, 2021. https://www.nshealth.ca/sites/nshealth.ca/files/feb10_contacttracing_eng_1.pdf. Accessed: 2020-10.

[37] Park, S. W., Bolker, B. M., Champredon, D., Earn, D. J. D., Li, M., Weitz, J. S., Grenfell, B. T., and Dushoff, J. Reconciling early-outbreak estimates of the basic reproductive number and its uncertainty: framework and applications to the novel coronavirus (SARS-CoV-2) outbreak. *Journal of The Royal Society Interface 17*, 168 (2020), 20200144. doi:10.1098/rsif.2020.0144.

[38] Phucharoen, C., Sangkaew, N., and Stosic, K. The characteristics of COVID-19 transmission from case to high-risk contact, a statistical analysis from contact tracing data. *EClinicalMedicine 27*, 100543 (Oct, 2020), 1–11. doi:10.1016/j.eclinm.2020.100543.

[39] Popa, A. A decision support system for optimizing the cost of social distancing in order to stop the spread of COVID-19. https://arxiv.org/abs/2004.02807, 2020.

[40] Rais, A., and Viana, A. Operations research in healthcare: a survey. *International Transactions in Operational Research 18*, 1 (2011), 1–31. doi:10.1111/j.1475-3995.2010.00767.x.

[41] Rausser, G. C., and Johnson, S. On the limitations of simulation in model evaluation and decision analysis. *Simulation & Games 6*, 2 (1975), 115–150. doi:10.1177/104687817500600201.

[42] Rawson, T., Brewer, T., Veltcheva, D., Huntingford, C., and Bonsall, M. B. How and when to end the COVID-19 lockdown: An optimization approach. *Frontiers in Public Health 8* (Jun, 2020), 262. doi:10.3389/fpubh.2020.00262.

[43] Risanger, S., Singh, B., Morton, D., and Meyers, L. A. Selecting pharmacies for COVID-19 testing to ensure access. *Health Care Management Science 24*, 2 (Jun, 2021), 330–338. doi:10.1007/s10729-020-09538-w.

[44] Ritchie, H., Ortiz-Ospina, E., Beltekian, D., Mathieu, E., Hasell, J., Macdonald, B., Giattino, C., and Roser, M. Coronavirus pandemic (COVID-19) – the data. https://ourworldindata.org/coronavirus. Accessed: 2020-09.

[45] Roche, B., Drake, J. M., and Rohani, P. An agent-based model to study the epidemiological and evolutionary dynamics of influenza viruses. *BMC Bioinformatics 12*, 1 (Mar, 2011), 87. doi:10.1186/1471-2105-12-87.

[46] Russell, T. W., Wu, J. T., Clifford, S., Edmunds, W. J., Kucharski, A. J., and Jit, M. Effect of internationally imported cases on internal spread of COVID-19: a mathematical modelling study. *The Lancet Public Health 6*, 1 (Jan, 2021), e12–e20. doi:10.1016/S2468-2667(20)30263-2.

[47] Statistics Canada. Table 13-10-0777-01 number and percentage of adults (aged 18 years and older) in the household population with underlying health conditions, by age and sex (two-year period). doi:10.25318/1310077701. Accessed: 2020-08.

[48] Statistics Canada. Table 17-10-0005-01 population estimates on July 1st, by age and sex. doi:10.25318/1710000501. Accessed: 2020-08.

[49] Statistics Canada. Table 24-10-0005-01 international travellers entering or returning to Canada, by province of entry, seasonally adjusted. doi:10.25318/2410000501. Accessed: 2020-09.

[50] Statistics Canada. Table 24-10-0027-01 number of domestic trips made by Canadian residents, by trip characteristics, inactive (x 1,000). doi:10.25318/2410002701. Accessed: 2020-09.

[51] Statistics Canada. Table 24-10-0042-01 provincial and territorial gross domestic product (GDP) and employment generated by tourism and related measures (x 1,000,000). doi:10.25318/2410004201. Accessed: 2021-01.

[52] Statistics Canada. Table 36-10-0434-01 gross domestic product (GDP) at basic prices, by industry, monthly (x 1,000,000). doi:10.25318/3610043401. Accessed: 2021-01.

[53] Tanner, M. W., Sattenspiel, L., and Ntaimo, L. Finding optimal vaccination strategies under parameter uncertainty using stochastic programming. *Mathematical Biosciences 215*, 2 (Oct, 2008), 144–151. doi:10.1016/j.mbs.2008.07.006.

[54] Teytelman, A., and Larson, R. C. Multiregional dynamic vaccine allocation during an influenza epidemic. *Service Science 5*, 3 (Sep, 2013), 197–215. doi:10.1287/serv.2013.0046.

[55] Toda, A. A. Susceptible-Infected-Recovered (SIR) dynamics of COVID-19 and economic impact. Papers, arXiv.org, Mar, 2020. https://EconPapers.repec.org/RePEc:arx:papers:2003.11221.

[56] Tuite, A. R., Fisman, D. N., and Greer, A. L. Mathematical modelling of COVID-19 transmission and mitigation strategies in the population of Ontario, Canada. *CMAJ 192*, 19 (2020), E497–E505. doi:10.1503/cmaj.200476.

[57] Uribe-Sánchez, A., Savachkin, A., and Santana, A. A predictive decision-aid methodology for dynamic mitigation of influenza pandemics. *OR Spectrum 33*, 3 (Jul, 2011), 751–786. doi:10.1007/s00291-011-0249-0.

[58] Victoria, G., Solis-Daun, J., and Zuñiga, L. D. Epidemiological discrete model for the expedited government decision-making in the face of the COVID-19 pandemic for closed populations. https://www.researchgate.net/publication/340682007_epidemiological_discrete_model_for_the_expedited_government_decision-making_in_the_face_of_the_covid-19_pandemic_for_closed_populations.

[59] Wang, D., Hu, B., Hu, C., Zhu, F., Liu, X., Zhang, J., Wang, B., Xiang, H., Cheng, Z., Xiong, Y., Zhao, Y., Li, Y., Wang, X., and Peng, Z. Clinical characteristics of 138 hospitalized patients with 2019 novel coronavirus–infected pneumonia in Wuhan, China. *JAMA 323*, 11 (2020), 1061–1069. doi:10.1001/jama.2020.1585.

[60] Wang, W., Li, Y., and Zhang, J. System dynamics modeling of sars transmission - a case study of Hebei province. In *2009 International Conference on Management and Service Science* (2009), pp. 1–4. doi:10.1109/ICMSS.2009.5303731.

[61] Yang, X., Yu, Y., Xu, J., Shu, H., Xia, J., Liu, H., Wu, Y., Zhang, L., Yu, Z., Fang, M., Yu, T., Wang, Y., Pan, S., Zou, X., Yuan, S., and Shang, Y. Clinical course and outcomes of critically ill patients with SARS-CoV-2 pneumonia in Wuhan, China: a single-centered, retrospective, observational study. *The Lancet Respiratory Medicine 8*, 5 (2020), 475–481. doi:10.1016/S2213-2600(20)30079-5.

[62] Yarmand, H., Ivy, J. S., Denton, B., and Lloyd, A. L. Optimal two-phase vaccine allocation to geographically different regions under uncertainty. *European Journal of Operational Research 233*, 1 (Feb, 2014), 208–219. doi:10.1016/j.ejor.2013.08.027.

[63] Zaric, G. S., Ed. *Operations Research and Health Care Policy*. International Series in Operations Research Management Science. Springer, 2013.

[64] Zhigljavsky, A., Fesenko, I., Wynn, H., Whitaker, R., Kremnizer, K., Noonan, J., and Gillard, J. A prototype for decision support tool to help decision-makers with the strategy of handling the COVID-19 UK epidemic. *medRxiv* (2020). doi:10.1101/2020.04.24.20077818.

Appendix A

Time-Based Optimization Strategies for Remaining Budgets

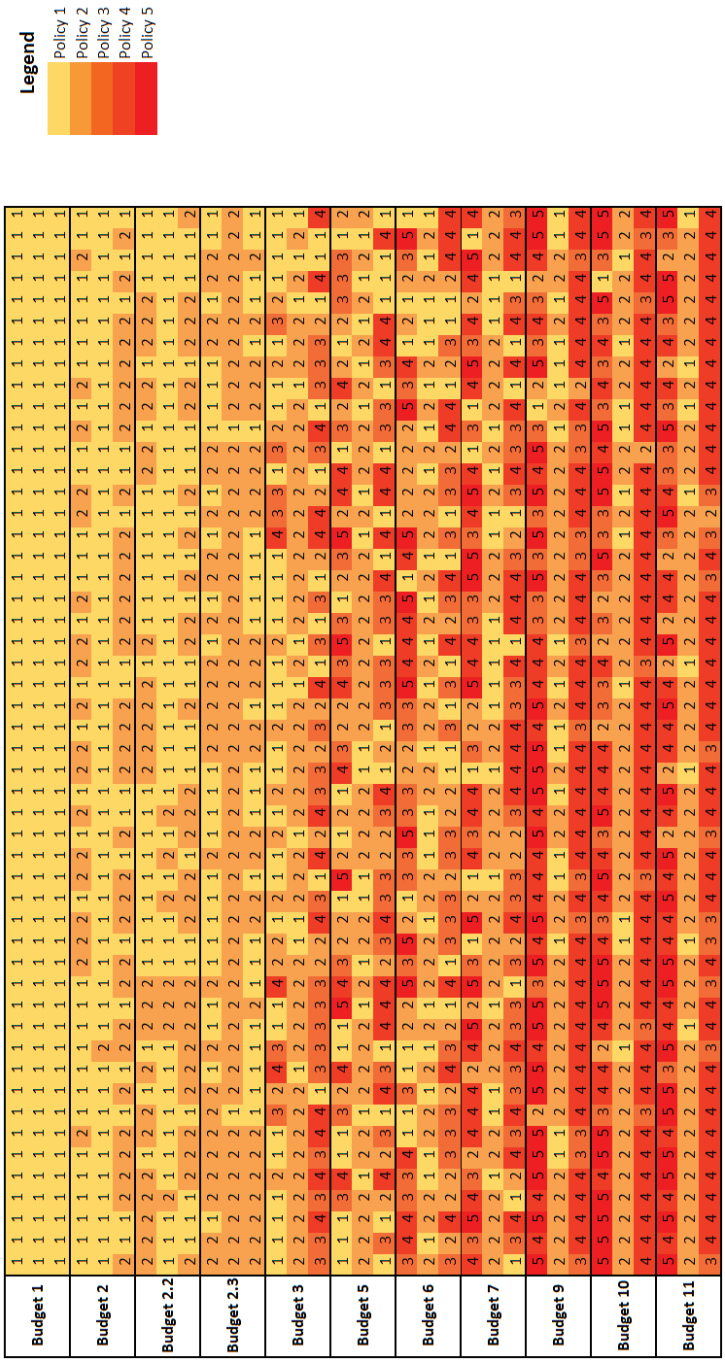

Appendix B

Time-Based Optimization Strategy Cost and Infections for Remaining Budgets

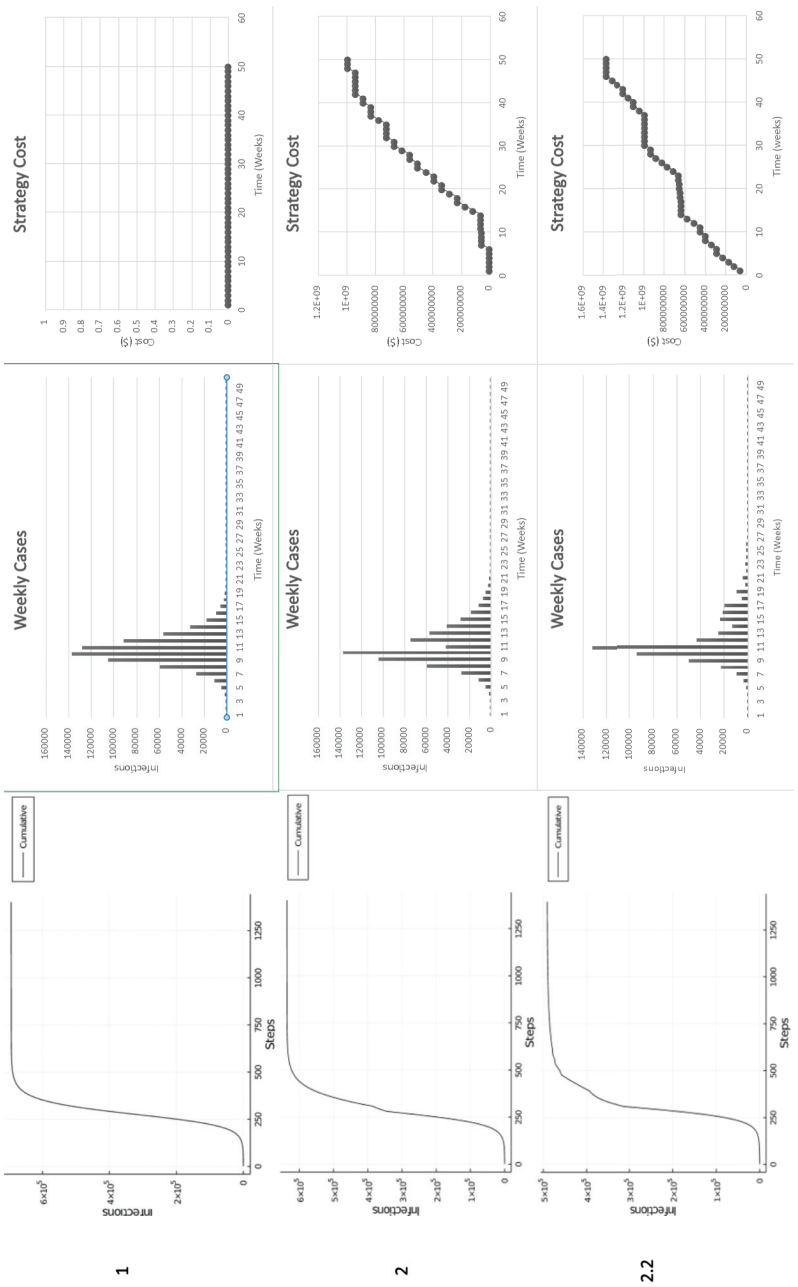

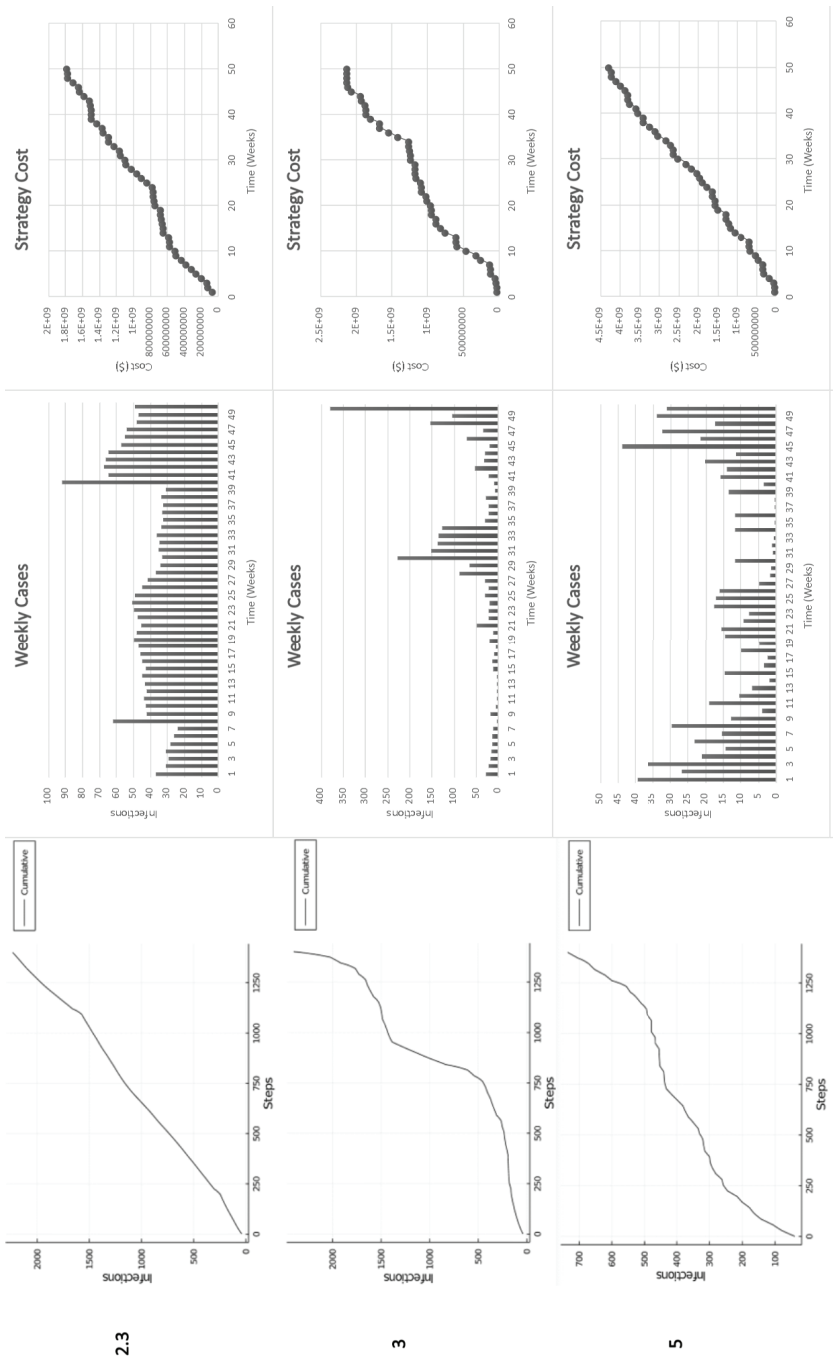
Strategy Cost
Cost ($)
Time (Weeks)
Weekly Cases
Infections
Time (Weeks)
Cumulative
Infections
Steps
2.3
3
5

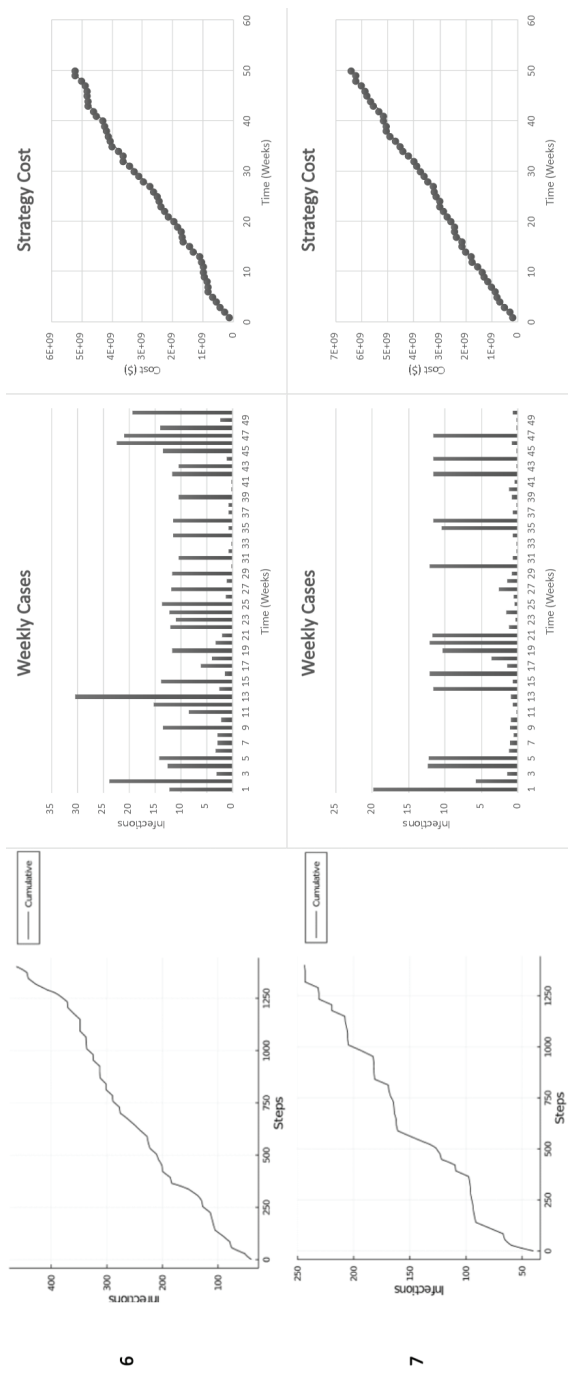
Strategy Cost
Cost ($)
Time (Weeks)
Weekly Cases
Infections
Time (Weeks)
Cumulative
Infections
Steps
6
7

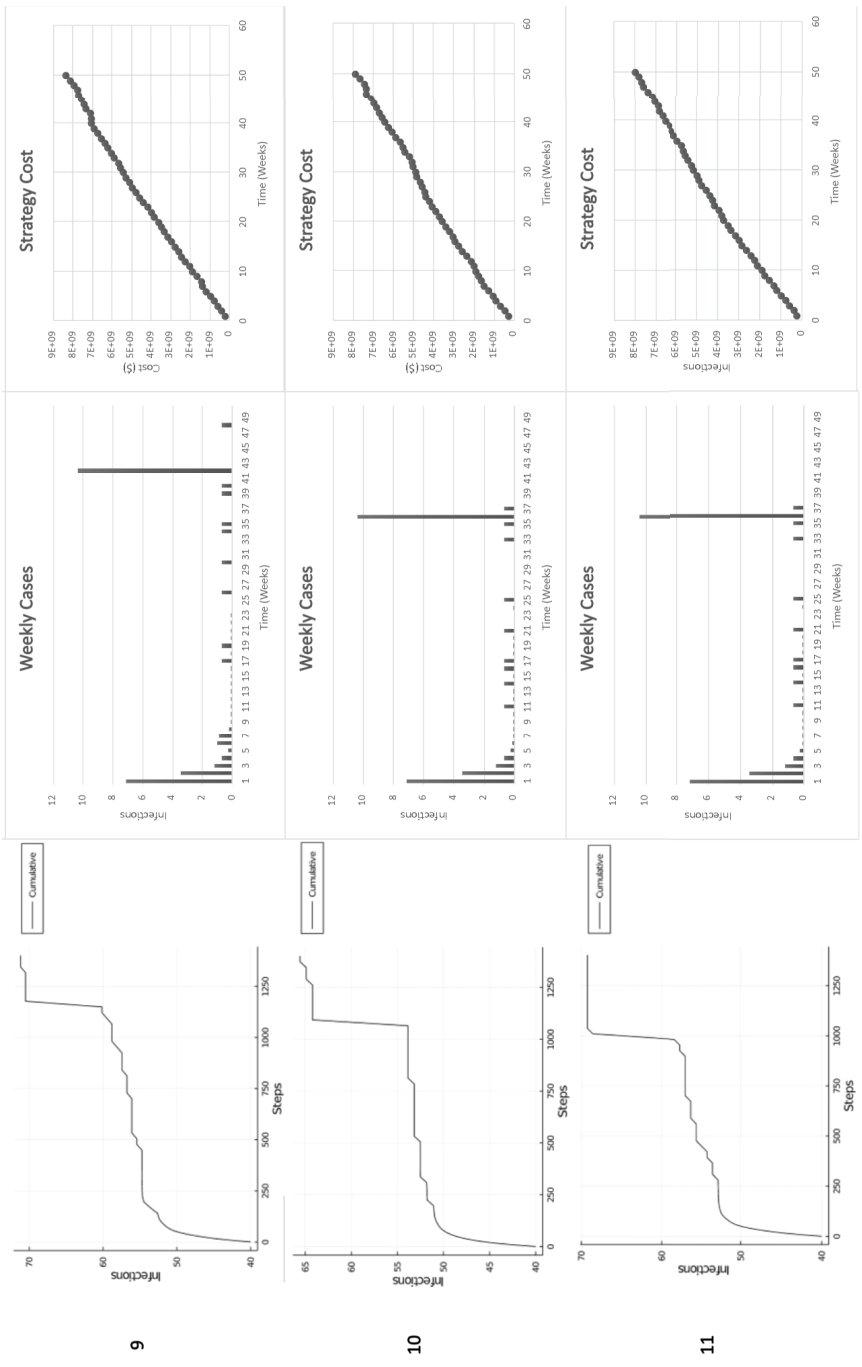
Strategy Cost
Cost ($)
Time (Weeks)
Weekly Cases
Infections
Time (Weeks)
Cumulative
Infections
Steps
9
10
11

Appendix C

Extended SA Results

UL12	LL21	UL23	LL32	UL34	LL43	UL45	LL54	UL56	LL65	Cost	Infections	Penalized Infections
13	11	30	17	42	21	44	6	42	12	724689222	1013	1013
13	11	30	17	42	21	44	5	42	12	724689222	1013	1013
13	11	30	17	42	21	44	5	42	12	724689222	1013	1013
13	12	30	17	42	21	43	5	42	12	716855354	1104	1104
14	12	30	17	41	22	43	5	41	12	876791077	1144	1144
14	12	31	17	41	22	43	4	41	12	876791077	1144	1144
14	12	31	17	41	22	43	4	41	12	876791077	1144	1144
14	12	31	17	41	22	43	4	40	12	876791077	1144	1144
14	12	31	17	41	22	43	5	40	12	876791077	1144	1144
13	12	30	17	41	22	43	5	40	12	876791077	1144	1144
13	12	30	17	41	22	43	5	40	12	876791077	1144	1144
13	12	30	17	41	22	43	5	39	12	876791077	1144	1144
14	13	30	17	41	21	43	5	39	12	716855354	1162	1162
14	12	29	17	41	21	43	5	39	12	716855354	1104	1104
14	12	29	17	41	22	43	5	39	12	876791077	1144	1144
14	12	29	18	41	22	43	4	39	12	821732649	1154	1154
14	12	29	18	40	22	43	4	39	12	821732649	1154	1154
14	12	28	18	41	22	43	4	38	11	821732649	1154	1154
14	12	28	18	41	22	43	4	38	11	821732649	1154	1154
14	12	29	18	41	22	43	4	38	11	821732649	1154	1154
14	11	29	18	41	22	43	4	38	12	829566517	1095	1095
14	11	29	18	42	22	43	5	38	12	829566517	1095	1095
15	11	30	18	41	22	43	5	38	12	829566517	1095	1095
15	11	30	17	42	22	44	5	38	12	884624945	1085	1085
16	11	30	17	42	22	44	5	39	12	884624945	1085	1085
17	11	30	17	42	22	44	6	39	12	884624945	1085	1085
17	11	30	17	42	21	44	7	39	11	724689222	1013	1013
17	11	30	16	42	21	44	7	39	11	724689222	1013	1013
17	10	30	16	42	21	44	6	39	12	732523090	928	928
17	10	30	16	43	21	43	5	39	12	732523090	928	928
17	10	30	16	43	21	44	5	39	13	732523090	928	928
17	10	30	16	44	21	44	5	39	13	732523090	928	928
17	11	30	16	44	22	44	5	39	14	884624945	1085	1085
17	11	30	16	44	21	44	5	39	14	724689222	1013	1013
17	12	30	15	44	21	44	6	39	14	771913782	1094	1094
17	13	30	16	44	21	44	6	39	13	716855354	1162	1162
17	12	30	17	44	21	44	5	39	14	716855354	1104	1104
16	11	29	17	44	21	45	5	40	14	724689222	1013	1013
16	11	29	17	43	21	45	5	40	14	724689222	1013	1013
15	12	30	17	43	21	45	5	41	14	716855354	1104	1104
15	12	30	17	43	22	46	5	41	14	876791077	1144	1144
15	12	30	17	43	23	47	5	41	14	876791077	1144	1144
15	11	29	18	43	23	47	5	41	14	829566517	1095	1095
15	11	29	18	43	23	47	5	41	14	829566517	1095	1095
15	11	29	19	43	23	46	5	41	14	829566517	1095	1095
15	11	29	19	42	23	46	4	41	14	829566517	1095	1095
14	11	29	19	42	23	46	4	41	14	829566517	1095	1095
14	11	30	19	42	23	45	4	41	14	829566517	1095	1095
14	12	30	19	42	23	44	4	41	14	821732649	1154	1154
14	13	30	19	41	23	45	5	41	15	821732649	1220	1220
14	13	30	19	40	22	45	6	41	15	821732649	1220	1220
14	12	30	19	40	22	45	6	41	15	821732649	1154	1154

UL12	LL21	UL23	LL32	UL34	LL43	UL45	LL54	UL56	LL65	Cost	Infections	Penalized Infections
14	12	31	19	40	22	44	6	41	15	821732649	1154	1154
14	12	31	19	41	22	44	6	41	16	821732649	1154	1154
14	12	31	20	41	22	44	7	41	17	766674221	1164	1164
14	12	31	19	41	22	44	7	41	17	821732649	1154	1154
14	13	31	19	42	21	44	7	41	17	716855354	1162	1162
14	13	31	19	42	21	45	7	41	17	716855354	1162	1162
14	13	31	20	42	22	45	7	41	17	766674221	1230	1230
14	13	31	20	42	22	46	7	41	18	766674221	1230	1230
14	13	31	20	42	22	46	7	41	18	766674221	1230	1230
14	12	31	20	43	23	45	8	42	15	766674221	1164	1164
14	12	31	20	43	23	45	7	42	15	766674221	1164	1164
14	12	31	21	43	23	46	6	41	16	766674221	1164	1164
14	12	30	21	43	23	46	6	41	15	766674221	1164	1164
13	12	30	20	43	24	46	6	41	15	766674221	1164	1164
14	12	40	12	52	20	58	21	37	13	826972210	1084	1084
13	12	40	12	52	20	58	20	37	13	826972210	1084	1084
14	13	39	12	51	18	59	21	38	12	826972210	1143	1143
14	13	39	13	51	18	59	21	38	13	771913782	1153	1153
14	13	39	13	52	17	59	21	38	13	771913782	1153	1153
14	12	40	13	53	17	59	21	39	12	771913782	1094	1094
14	11	40	13	53	17	58	21	39	12	779747650	1004	1004
14	11	40	13	53	18	59	21	40	11	779747650	1004	1004
14	11	39	12	53	18	60	21	39	12	834806078	994	994
13	11	39	12	54	18	60	20	39	12	834806078	994	994
14	11	40	12	55	18	60	19	39	13	834806078	994	994
13	11	40	12	55	18	60	20	39	13	834806078	994	994
12	11	40	11	54	17	60	21	39	13	889864506	984	984
12	10	41	11	54	17	60	21	39	13	897698374	899	899
12	10	41	11	54	16	60	21	39	13	897698374	899	899
12	10	42	11	54	16	60	21	38	13	897698374	899	899
11	10	42	11	54	16	60	22	38	13	897698374	899	899
11	10	42	11	54	16	61	21	38	13	897698374	899	899
11	10	42	10	54	16	61	21	39	13	952756802	889	889
11	10	42	10	55	16	62	21	39	13	952756802	889	889
11	10	41	10	55	16	62	20	39	14	952756802	889	889
11	10	41	9	55	16	62	20	40	14	1.008E+09	879	22801
12	10	41	9	56	16	62	20	40	14	1.008E+09	879	22840
12	11	41	9	56	17	62	20	39	14	999981362	965	965
12	11	41	9	56	17	62	20	39	14	999981362	965	965
12	11	42	9	56	17	62	20	39	14	999981362	965	965
12	11	42	9	56	17	62	20	39	14	999981362	965	965
12	11	42	9	56	16	62	20	39	14	999981362	965	965
12	11	42	9	56	16	62	20	39	14	999981362	965	965
12	11	43	9	55	16	62	19	39	14	999981362	965	965
12	11	43	9	55	16	62	19	39	14	999981362	965	965
12	11	43	9	55	16	62	19	40	14	999981362	965	965
12	11	43	10	56	16	62	19	40	14	944922934	975	975
12	10	43	10	55	16	62	20	40	14	952756802	889	889
11	9	42	10	55	16	61	20	40	14	952756802	889	889
11	9	42	10	55	16	61	19	40	13	952756802	889	889
11	9	42	10	55	15	61	19	41	13	952756802	889	889
11	8	42	10	55	15	61	19	41	13	952756802	889	889